*J. Nannoplankton Res.* **37** (2–3), 2017, pp.77–112 © 2017 International Nannoplankton Association
ISSN 1210-8049 Printed by The Sheridan Press, USA


# Oligocene-Pliocene taxonomy and stratigraphy of the genus *Sphenolithus* in the circum North Atlantic Basin: Gulf of Mexico and ODP Leg 154

## Jim Bergen*
Paleo at the Hill Country, Brenham, TX 77833, USA; *jbnanno@att.net

## Eric de Kaenel
DPR, chemin sous la Roche 4b, 1185 Mont-sur-Rolle, Switzerland; edekaenel@bluewin.ch

## Stacie Blair
Blair Biostratigraphy, 13126 Park Forest Trail, Cypress, TX 77429; stacie.blair81@gmail.com

## Todd Boesiger
ALS Global, 5929 Lee Circle, Lincoln, NE 68506; tboesig@gmail.com

## Emily Browning
BP America, RD-Exploration NWD, 200 Westlake Park Blvd, Houston, TX 77079; Emily.Browning@bp.com

Manuscript received 12th September, 2016; revised manuscript accepted 20th May, 2017

**Abstract** *Sphenolithus* is secondary only to the genus *Discoaster* in Cenozoic nannofossil biostratigraphy, notably of primary importance for the Oligocene to Early Miocene. The research presented herein provides a framework for Oligocene to Middle Pliocene *Sphenolithus*, where gradations between individual taxa and their stratigraphic ranges are presented. Integration of schemes from BP, Amoco and Arco Vastar, to form a single composite Neogene calcareous nannofossil framework for the Gulf of Mexico basin, began around the turn of the century with focus on refining taxonomic concepts to solve stratigraphic discrepancies between the heritage schemes. Further study and bioevent calibration was accomplished through analyses of deep-water wells in the Gulf of Mexico along with research grounding the integrated framework to the "astronomical clock" of ODP Leg 154 back into the middle Early Oligocene at an average sample resolution of 21 kyr. Forty-two species are considered herein, in addition to the morphologically-similar *Ilselithina fusa*. Thirteen new species are introduced. *Sphenolithus peartiae* and *Sphenolithus distentus* are emended. Clarification of taxonomic concepts by the use of morphologic groups is supplemented with identification tables, drawings, and light photomicrographs. Iterative processes, in terms of size, are stressed.

**Keywords** *Sphenolithus*, nannofossils, Oligocene, Miocene, taxonomy, Gulf of Mexico

## 1. Introduction

One of the major achievements in biostratigraphy within BP after the mergers with Amoco and Arco Vastar was the integration of the Cenozoic calcareous microfossil biostratigraphies for the Gulf of Mexico (GoM) Basin, which were developed independently within the three heritage companies. The resulting Neogene framework, with a biostratigraphic resolution of 141 kyr is, to our knowledge the only fully astronomically-tuned industrial framework. A twelve-year research program on Ocean Drilling Program (ODP) Leg 154 on the Ceará Rise in the western equatorial Atlantic (Figure 1) provided a cyclostratigraphic-based age model for the Early Oligocene (30.679Ma) through Early Pleistocene (1.595Ma). This internal research program also included work on the Oligocene-Miocene boundary Global Stratotype Section and Point (GSSP) in Italy (de Kaenel & Bergen, 2008; Bergen *et al*., 2009; de Kaenel & Villa, 2010). Research on the Leg 154 material was conducted at an average sample resolution that approximates that of a precession cycle. The details of our age model with sample depths and ages will be presented in Bergen *et al.* (in prep.).

We consider taxonomic clarification of species necessary before publication of the astronomically-tuned BP Gulf of Mexico Neogene chronostratigraphic chart (GNATTS). The realization of the need for more precise and standard taxonomic concepts in the Gulf of Mexico was first demonstrated by a taxonomic working group formed in late 1990's to discuss the genus *Pseudoemiliania* and the *Discoaster quinqueramus* lineage. The series of five manuscripts produced for this volume are loosely organized around the taxonomic groupings considered by a second industrial nannofossil working group (the Gulf Coast Taxonomic Equivalency Project), focused on the GoM Miocene, which convened three times in Houston from 2011 to 2012. Our five papers are focused on the

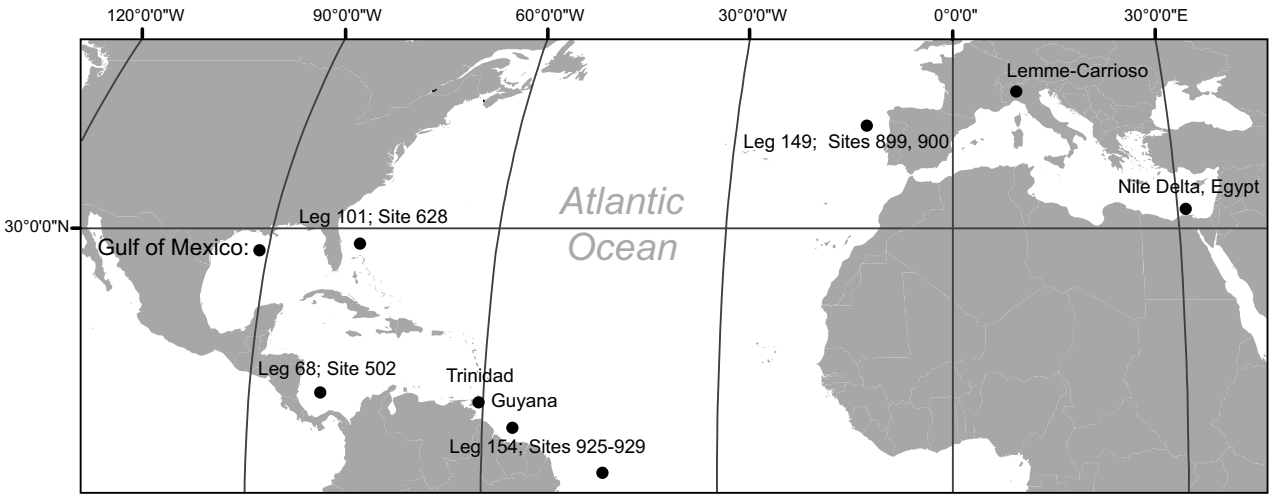


**Figure 1:** Locality map of materials used in this publication

stratigraphically-significant genera *Helicosphaera*, *Sphenolithus,* and *Discoaster* (three papers) and introduce BP-heritage GoM taxonomy and stratigraphy for the first time. Other taxa significant to the Gulf of Mexico Neogene discussed in these papers include the genera *Amaurolithus*, *Calcidiscus*, *Camuralithus, Catinaster*, *Ceratolithus*, *Coccolithus, Coronocyclus*, *Cryptococcolithus, Cyclicargolithus*, *Dictyococcites, Ilselithina*, *Minylitha* and *Reticulofenestra*.

## 2. Materials and methods

Lithic materials used for this study are from outcrop, core, and well cuttings. ODP Leg 154 collections at the International Ocean Discovery Program (IODP) repository in Bremen (Germany) provided the main source of public core material. Other collections used were: (1) DSDP Leg 68 (Hole 502) in the western Caribbean Sea; (2) ODP Leg 149 (Holes 899B & 900A) in the northeastern Atlantic Ocean; (3) ODP Leg 101 (Hole 628A) in the western North Atlantic Ocean; (4) the base Neogene GSSP section near Lemme-Carrioso in northern Italy; and (5) the Trinidad "Bolli collection" sampled by H.M. Bolli (1957) (See Figure 1). Many important Oligocene-Miocene nannofossil taxa have been published from the Bolli collections (Bramlette & Riedel, 1954; Bramlette & Wilcoxon, 1967; Bukry, 1971b; Bukry & Percival, 1971; Gartner, 1967; Hay *et al*., 1967; Martini & Bramlette, 1963; Roth, 1970), but none in the past 45 years. Three Trinidad samples are used herein: (1) JS 20, *Globorotalia opima opima* Zone, Zone NP24; (2) KR9397, *Catapsydrax stainforthi* Zone, Zone NN3; and (3) Bo267, *Catapsydrax dissimilis* Zone, Zone NN2. Deep-water Gulf of Mexico well materials came predominantly from ditch-cutting samples. Specimens photographed from wells in Guyana and the Nile Delta, Egypt are also illustrated.

The following stratigraphic abbreviations are used: LO (lowest occurrence) and HO (highest occurrence); abundance modifiers are: R (regular) for LRO and HRO, F (few) for LFO and HFO, C (common) for LCO and HCO.

The objective of this work is to clarify taxonomic concepts and present the GoM stratigraphy developed over the past five decades from the three BP heritage companies (Amoco, Arco Vastar and BP), not to compare our results to other published stratigraphies of the GoM Basin or research on ODP Leg 154. The geologic ages derived from sampling of ODP Leg 154 are maintained at three decimal precision through the manuscript for consistency; error given on ages is the difference in age for the next sample analyzed upwards or downwards in the composite section. Links to supplementary materials will be provided on the publication's website and include biometrics (http://ina.tmsoc.org/JNR/JNR-contents.htm).

## 3. Biostratigraphy

The primary zonation (NP/NN Zones) referred to herein is Martini (1971), although the zonation (CP/CN Zones) of Okada & Bukry (1980) is also referred to within the text. Any new zones or emendations are presented by de Kaenel *et al*. (2017) and Blair *et al*. (2017) in this volume.

Four *Sphenolithus* species are used in zonal definitions for the Lower Oligocene to lower Middle Miocene (NP23-NN5): *S. ciperoensis*, *S. distentus*, *S. belemnos* and *S. heteromorphus*. The LO of *S. ciperoensis* defines the base of Zone NP24 and its age is determined with high reliability from Leg 154 by both de Kaenel and Bergen. We believe discrepancies in this age determination (see Aubry, 2014) are largely taxonomic, although the holotype is clearly illustrated. Conversely, the holotype of *S. distentus* is highly problematic, making taxonomic clarification necessary for accurate zonal determinations. Its LO defines the base of Zone CP18, which subdivides Zone NP23; its HO defines the base of Zone NP25 (also base Subzone CP19b). The top of Zone NP25, defined by the HO of *S. ciperoensis*, is easily delineated because it represents the extinction of the lanceolate sphenoliths. A Zone NP26, defined by de Kaenel *et al*. (2017) from

| Taxon | Event | Zone Martini 71 | Age (Ma) | Error$_1$ (Ma) | Rel$_2$ | Hole-Core-Sec. cm-cm | Depth (rmcd)$_3$ |
|---|---|---|---|---|---|---|---|
| *S. abies* | HO | NN16 | 3.510 | 0.017 | 10 | 926C-11H-2, 138-139 | 108.85 |
| *S. moriformis* | HO | NN16 | 3.531 | 0.008 | 10 | 926C-11H-3, 55-56 | 109.52 |
| *S. neoabies* | HO | NN16 | 3.531 | 0.008 | 10 | 926C-11H-3, 55-56 | 109.52 |
| *S. abies* | HFO | NN16 | 3.666 | 0.019 | - | 926C-11H-6, 30-31 | 113.77 |
| *S. heteromorphus* | **HO** | **top NN5** | 13.408 | 0.028 | **10** | 926A-29-2, 99-101 | 292.19 |
| *S. heteromorphus* | LCO | NN4 | 17.383 | 0.010 | - | 928B-28-1, 0-2 | 272.64 |
| *S. apoxis* | HO | NN4 | 17.347 | 0.009 | 10 | 928B-27-CC, 30-32 | 271.42 |
| *S. apoxis* | HFO | NN4 | 17.425 | 0.018 | - | 928B-28-1, 110-111 | 273.74 |
| *S. heteromorphus* | LFO | NN4 | 17.652 | 0.020 | - | 928B-28-4, 55-57 | 277.69 |
| *S. belemnos* | **HO** | **top NN3** | 17.683 | 0.011 | **5** | 928B-28-4, 117-118 | 278.31 |
| *S. heteromorphus* | LO | NN3 | 17.791 | 0.020 | **9** | 928B-28-6, 40-41 | 280.54 |
| *S. belemnos* | HRO | NN3 | 17.831 | 0.020 | **10** | 928B-28-6, 118-119 | 281.32 |
| *S. procerus* | HO | NN3 | 18.612 | 0.020 | 9 | 926B-37-4, 90-92 | 371.42 |
| *S. paratintinnabulum* | HO | NN3 | 18.612 | 0.020 | 9 | 926B-37-4, 90-92 | 371.42 |
| *S. dissimilis* | HO | NN3 | 18.768 | 0.015 | 6 | 926B-38-1, 70-72 | 376.31 |
| *S. disbelemnos* | HO | NN3 | 18.768 | 0.015 | 9 | 926B-38-1, 70-72 | 376.31 |
| *S. calyculus* | HO | NN3 | 19.331 | 0.018 | **5** | 926B-39-5, 95-96 | 392.26 |
| *S. belemnos* | **LO** | **top NN2** | 19.414 | 0.019 | **7** | 926C-39-6, 30-31 | 394.52 |
| *S. cometa* | HRO | NN2 | 19.832 | 0.020 | **6** | 926B-41-1, 65-66 | 404.86 |
| *S. conicus* (>7) | INC | NN2 | 20.291 | 0.020 | - | 926B-42-3, 5-6 | 416.96 |
| *S. microdelphix* | HO | NN2 | 21.362 | 0.020 | **5** | 926B-45-5, 80-81 | 449.71 |
| *S. disbelemnos* | HCO | NN2 | 22.067 | 0.020 | - | 928B-35-2, 125-126 | 342.89 |
| *S. disbelemnos* | LCO | NN2 | 22.288 | 0.019 | - | 926B-48-4, 120-122 | 477.61 |
| *S. dissimilis* | LO | NN2 | 22.658 | 0.019 | 6 | 926B-49-5, 50-51 | 488.02 |
| *S. capricornutus* | HO | NN1 | 22.998 | 0.020 | 6 | 926B-50-4, 90-92 | 496.61 |
| *Sphenolithus spp.* | ACME | NN1 | 22.998 | 0.020 | - | 926B-50-4, 90-92 | 496.61 |
| *S. delphix* | HO | NP26 | 23.093 | 0.021 | 10 | 926B-50-6, 45-46 | 499.17 |
| *S. conicus* | ACME | NP26 | 23.253 | 0.019 | - | 926B-51-2, 115-116 | 503.46 |
| *S. ciperoensis* | HO | **top NP25** | 24.215 | 0.022 | 10 | 926B-53X-5, 70-71 | 526.72 |
| *S. bulbulus* | HO | NP25 | 24.248 | 0.015 | **4** | 926B-53X-5, 143-145 | 527.44 |
| *S. capricornutus* | LO | NP25 | 24.281 | 0.023 | **5** | 926B-54X-1, 1-2 | 529.73 |
| *S. bulbulus* | HRO | NP25 | 24.365 | 0.019 | 10 | 926B-54-2, 65-66 | 531.87 |
| *S. avis* | HO | NP25 | 24.408 | 0.043 | 5 | 926B-54-3, 30-31 | 533.02 |
| *S. ciperoensis* | HCO | NP25 | 24.456 | 0.048 | - | 926B-54-3, 145-146 | 534.17 |
| *S. peartiae* | HO | NP25 | 24.683 | 0.019 | **8** | 926B-55-1, 80-81 | 540.12 |
| *S. triangularis* | HO | NP25 | 24.700 | 0.017 | **8** | 928B-41-5, 75-76 | 403.33 |
| *S. ciperoensis* (>6) | HO | NP25 | 24.800 | 0.041 | **5** | 926B-55-3, 60-61 | 542.92 |
| *S. tawfikii* | HO | NP25 | 25.047 | 0.029 | 3 | 925A-26-4, 70-71 | 568.05 |
| *S. distentus* | **HO** | **top NP24** | 26.126 | 0.016 | **7** | 926B-58-7, 13-14 | 577.44 |
| *S. avis* | HRO | NP24 | 26.627 | 0.040 | **8** | 926B-60-3, 5-6 | 590.77 |
| *S. predistentus* | HO | NP24 | 26.926 | 0.041 | **10** | 926B-61-3, 20-21 | 600.62 |
| *S. peartiae* (>7) | HO | NP24 | 27.218 | 0.048 | **10** | 926B-62X-2, 133-134 | 609.84 |
| *S. pseudoradians* | HO | NP24 | 28.092 | 0.045 | **4** | 926B-64X-4, 75-76 | 631.56 |
| *S. apoxis* (>8) | HO | NP24 | 28.092 | 0.045 | **6** | 926B-64X-4, 75-76 | 631.56 |
| *S. akropodus* (<8) | HO | NP24 | 28.655 | 0.043 | **7** | 928B-50X-2, 5-6 | 485.49 |
| *S. ciperoensis* (>6) | LO | NP24 | 28.683 | 0.050 | **5** | 928B-50X-2, 52-53 | 485.96 |
| *S. akropodus* (<8) | HRO | NP24 | 29.127 | 0.039 | **10** | 925A-38R-6, 38-39 | 687.42 |
| *S. ciperoensis* | LO | **top NP23** | **29.171** | 0.027 | **10** | 925A-38R-7, 15-16 | 688.69 |
| *S. akropodus* | HO | NP23 | 29.294 | 0.046 | 9 | 925A-39R-2, 82-83 | 691.76 |
| *S. avis* | LO | NP23 | 30.512 | 0.033 | **1** | 925A-44R-2, 55-56 | 730.09 |

**Table 1:** Main *Sphenolithus* events for Gulf of Mexico (ages direct from our Leg 154 research). $_1$error is age of next sample. $_2$reliability index is number occurrences in top or bottom 10 samples (boldface = 2 researchers). $_3$revised measured composite depth (meters). NOTE: internal research on Leg 154 down to 30.679Ma

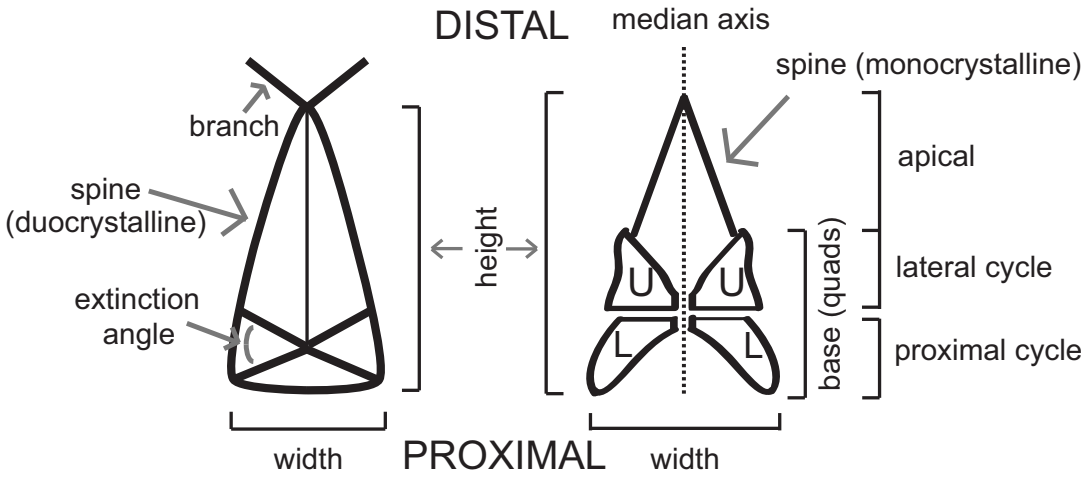


**Figure 2:** Sphenolith morphologic terms. U = upper, L = lower

the HO of *S. ciperoensis* up to the LO of medium-sized (≥ 10 to < 15$\mu$m) *Discoaster druggii,* is coincident with the Oligocene-Miocene boundary and dated at 23.030Ma in Leg 154. The total range of *S. belemnos* is used to define the limits of Zone NN3 herein, as the HO of *Triquetrorhabdulus carinatus* (base NN3) is diachronous within the Gulf of Mexico. The LO of *S. heteromorphus* may be used to subdivide Zone NN3, as it is the marker for the base of Zone CN3 of Okada & Bukry (1980). The base of Zone NN6, defined by the HO of *S. heteromorphus*, represents the extinction of conical sphenoliths with monocrystalline spines. Only four significant datum's recognized herein (Table 1) occur after extinction of *S. heteromorphus*, all of which are placed in proximity to the base of the Middle Pliocene.

## 4. Systematic Paleontology

Size variation through time is an iterative process well demonstrated by the genus *Sphenolithus*. The axiom for size is that the larger variants have shorter stratigraphic ranges within the range of the species. In this study, eight taxa proved to have stratigraphically significant size variants, one of which is described herein as a new species. *Sphenolithus microdelphix* is separated as a new species because of its relevance to the recognition of the Oligocene-Miocene boundary. Size variants among existing species include *S. celsus* - *S. predistentus*. Size categories follow those defined by Young *et al.* (1997).

Morphologic terms used herein are shown in Figure 2. Aubry (2014) provided an excellent synopsis of the genus; her five main morphologic groupings are followed herein with the exception of her elongate group, replaced here with a sphaeroconical group (Table 2). Aubry (2014) also distinguished two basic types of apical spines (ortholithid and heliolithid) important to her recognition of groups and subgroups. Instead, three basic types of apical spines are recognized herein, following Young *et al*. (1997): (1) compound; (2) monocrystalline; and (3) duocrystalline. *Ilselithina fusa* is considered because it is morphologically similar to the sphaeroconical group with which it shares having large proximal elements (i.e. a small number of elements per cycle). Forty-two sphenolith taxa are considered; about half of these taxa are classified as conical (Group 2), which is divided into six subgroups (Table 2). Drawings of the taxa belonging to Groups 1–4 are shown in Figure 3 and with their ranges in Figures 4 and 5. These drawings were rendered from light photomicrographs; they were based on holotypes, when possible.

| Grp. No. | GROUP NAME | PERIPHERAL OUTLINE | | ELEMENT SIZE | APICAL SPINE TYPE | PROXIMAL CYCLE | No. Taxa |
|---|---|---|---|---|---|---|---|
| 1 | *moriformis* | **hemispherical** | | medium | compound | | 5 |
| 2A | *abies* | CONICAL | conical | medium | compound | | 4 |
| 2B | *dissimilis* | CONICAL | **cylindro**conical | medium | compound | | 5 |
| 2C1 | *belemnos* | CONICAL | conical | medium | monocrystalline | narrow | 2 |
| 2C2 | *calyculus* | CONICAL | conical | medium | monocrystalline | equant | 3 |
| 2C3 | *delphix* | CONICAL | conical | medium | monocrystalline | flared | 3 |
| 2C4 | *heteromorphus* | CONICAL | conical | medium | monocrystalline | broad | 2 |
| 3 | *capricornutus* | biconical (**flaring**) | | medium | compound | | 3 |
| 4 | *umbrellus* | **sphaeroconical** | | large | variable | rounded | 3 |
| 5 | *ciperoensis* | **lanceolate** | | small | duocrystalline | | 12 |

**Table 2:** Morphologic groupings of Oligocene-Pliocene *Sphenolithus*. The bold type-face and shading emphasize important morphological characteristics that separate groupings

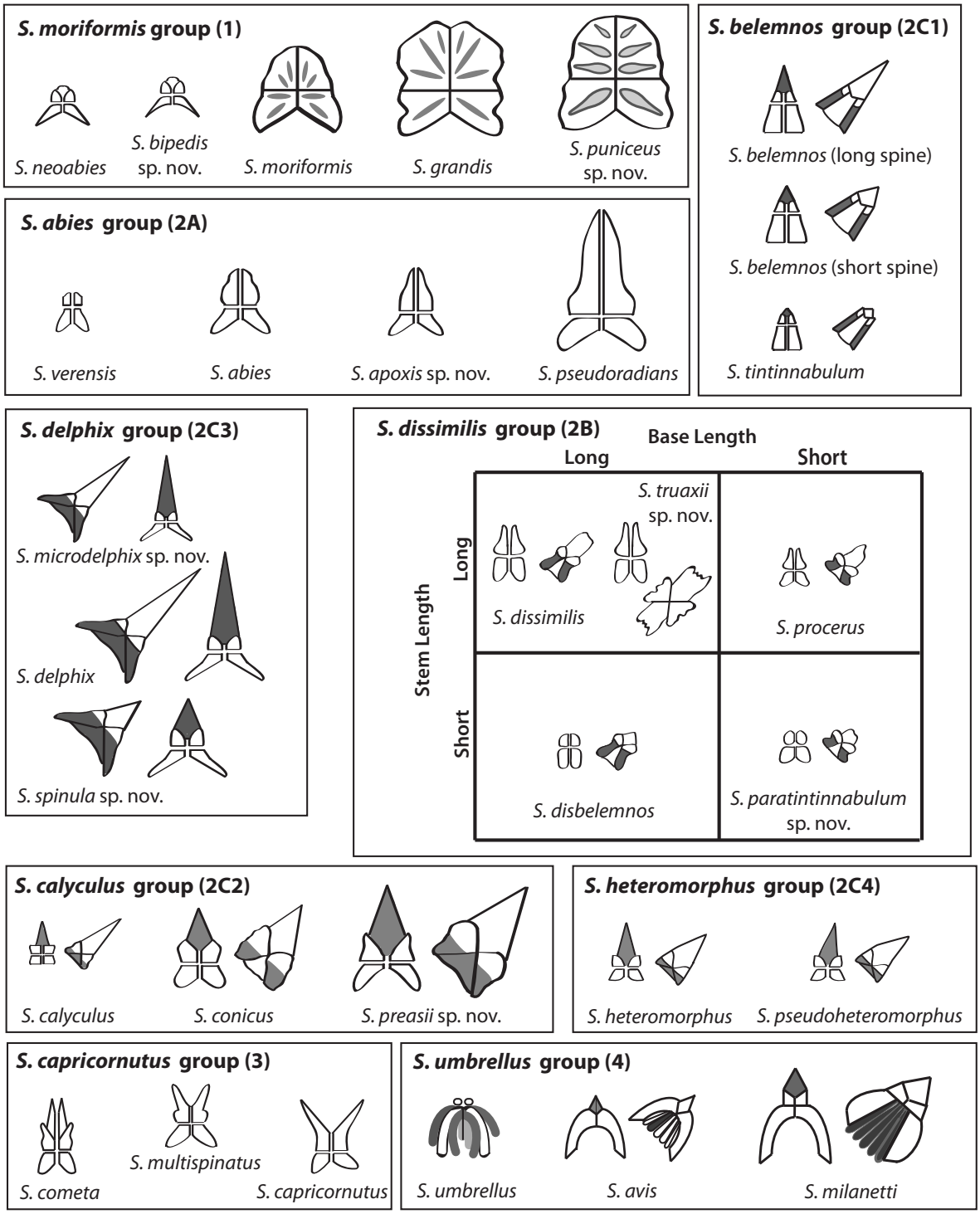


**Figure 3:** Schematics of *Sphenolithus* taxa for morphologic Groups 1-4

## 4.1 *Sphenolithus moriformis* group

This group is defined by their hemispherical lateral outlines. The five species included in this group are differentiated by their size, birefringence, and proximal cycle morphology (Table 3).

***Sphenolithus neoabies*** Bukry & Bramlette, 1969
Pl. 1, figs 1–4

1969 *Sphenolithus neoabies*, Bukry & Bramlette, p. 140, pl. 3, figs. 9–11.

**Remarks:** Bukry & Bramlette (1969) noted the small size of the species (2–4$\mu$m). The flared proximal cycle of the holotype is also considered diagnostic, which results in height to width ratios of less than 1 (holotype: 0.71). The indented proximal surface appears linear in cross-polarized light (XPL).

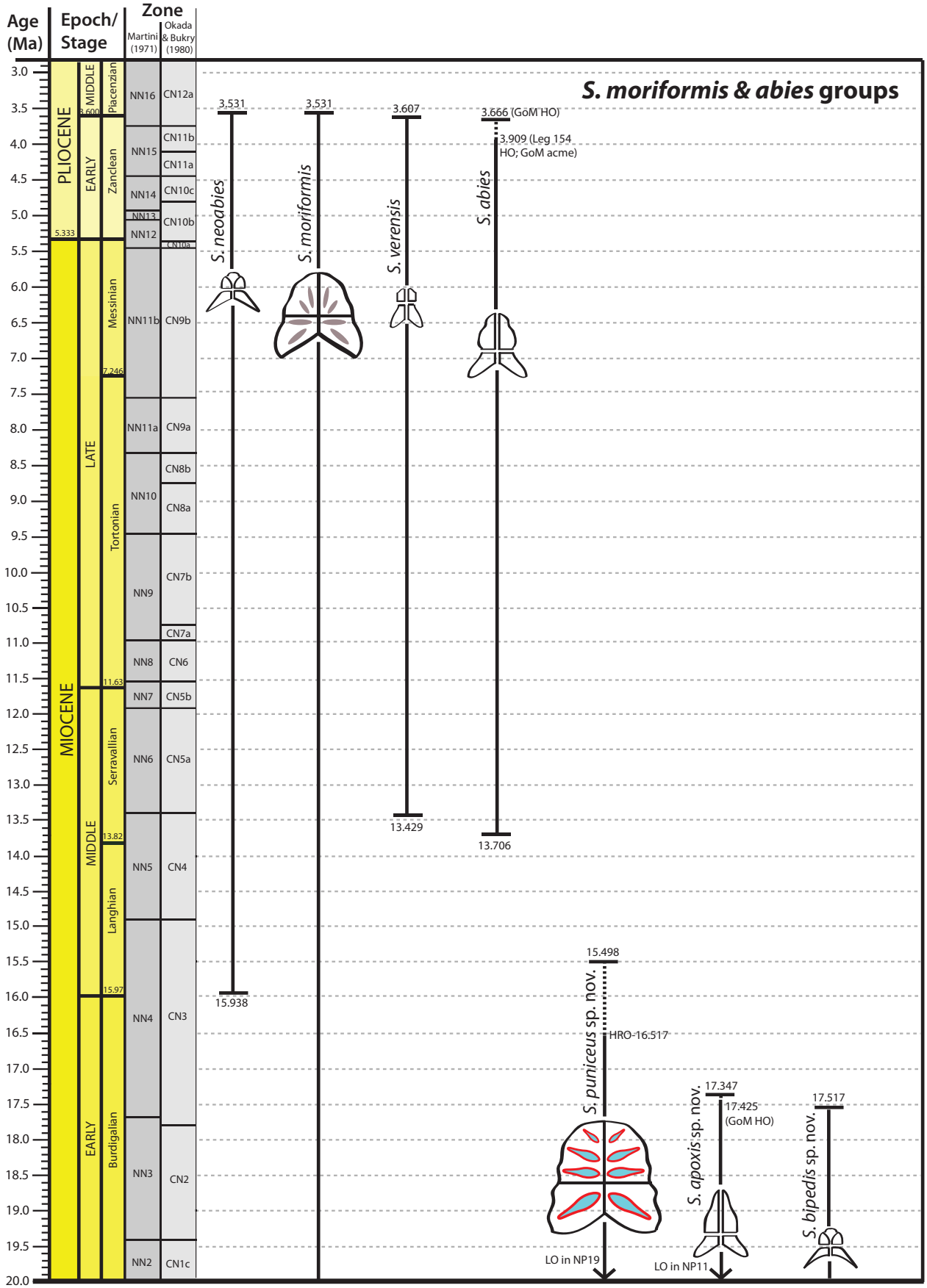


**Figure 4:** Range diagram of *Sphenolithus moriformis* (1) and *S. abies* (2A) morphologic groups

**Occurrence:** *Sphenolithus neoabies* ranges from lower Middle Miocene (NN4) to basal Middle Pliocene (NN16). The HO of *S. neoabies*, along with that of *S. moriformis*, represent the extinction of the genus in the GoM. This event is dated in Leg 154 research at 3.531Ma (Table 1). The LO of *S. neoabies* is also well-constrained in the Leg 154 research, placed in Sample 925C-38-3, 135–136cm and dated at 15.938Ma (0.020Ma error).

### *Sphenolithus bipedis* Bergen & de Kaenel, *sp. nov.*

Pl. 1, figs 5–12

**Derivation of name:** from Latin *bi*, meaning two and *pedis*, meaning foot.

**Diagnosis:** Hemispherical sphenolith with a flared proximal cycle and arcuate proximal surface.

**Description:** Very small to medium hemispherical sphenolith having a compound apical spine. Proximal cycle is laterally-extended or "flared", resulting in height to width ratios of less than 1 (0.81–0.91 for five measured specimens). Proximal surface strongly concave and arcuate. Size: 2.8–6.4$\mu$m (holotype: Length [L] = 2.4$\mu$m; width [W] = 2.8$\mu$m).

**Remarks:** *S. neoabies* is a younger and generally smaller version of *S. bipedis*. Their stratigraphic ranges are separated by approximately 1.58 million years in the ODP Leg 154 materials. The proximal surface of *S. bipedis* is more arcuate than the more linear and less concave proximal surface of *S. neoabies*. Other hemispherical sphenoliths do not possess a flared proximal cycle. *S. bipedis* has been referred to as "*S. delphix* (no stem)" in the BP GoM lexicon.

**Holotype:** Pl. 1, figs 5–6

**Type locality:** ODP Leg 154, Hole 929A, Ceará Rise, western equatorial Atlantic

**Type level:** Sample 35-3, 125–27cm (23.155Ma), Zone NP26, Upper Oligocene

**Occurrence:** In Leg 154, the LO of *S. bipedis* was placed in Sample 925A-38R3, 70–71cm within Zone NP24 and dated at 28.971Ma (error 0.041Ma), but it is possible the species could range down into Zone NP23. In Leg 154, the HO is well-constrained within lower Zone NN4 in Sample 928B-28-2, 115–116cm and dated at 17.517Ma (0.022Ma error).

### *Sphenolithus moriformis* (Brönnimann & Stradner, 1960) Bramlette & Wilcoxon, 1967

Pl. 1, figs 13–18

1960 *Nannoturbella moriformis* Brönnimann & Stradner (*pro parte*), p. 368, figs. 11–13, 16, *non* figs. 14–15.

1967 *Sphenolithus moriformis* (Brönnimann & Stradner) Bramlette & Wilcoxon (*pro parte*), p. 124, pl. 3, figs. 1–4, *non* figs. 5–6.

**Remarks:** The Lower Eocene holotype has a hemispherical lateral outline, whereas the conical specimen illustrated by Brönnimann & Stradner (1960) is not included within this species concept; neither is the conical specimen illustrated by Bramlette & Wilcoxon (1967). *Sphenolithus moriformis* is distinguished from *S. puniceus* sp. nov. by being less birefringent. Haq & Berggren (1978) distinguished *S. grandis* from *S. moriformis* by its larger size and more disjoined elements.

**Occurrence:** *S. moriformis* is the last surviving species of *Sphenolithus* in the GoM and its earliest Middle Pliocene extinction has been calibrated in Leg 154 (Table 1).

### *Sphenolithus puniceus* Bergen & de Kaenel, *sp. nov.*

Pl. 1, figs 19–26

**Derivation of name:** from Latin *puniceus*, meaning purplish-red.

**Diagnosis:** A highly birefringent (first order blue to red interference colors) hemispherical sphenolith.

**Description:** Medium to large, hemispherical sphenolith with a compound apical spine. The species is distinguished by its very high birefringence - exhibiting first order blue to red interference colors at its core in both plan and lateral view. Height to width ratio = 0.94–1.08 on three measured specimens. Size (six specimens): 6.8–11.2$\mu$m (holotype: L = 8.6$\mu$m; W = 8.0$\mu$m).

**Remarks:** *S. moriformis* and *S. grandis* also have hemispherical lateral outlines and compound apical spines, but do not display high first order blue to red birefringence.

**Holotype:** Pl. 1, figs 21–22

**Type locality:** ODP Leg 154, Hole 926B, Ceará Rise, western equatorial Atlantic

**Type level:** Sample 42-4, 35–37cm (20.350Ma), Zone NN2, Lower Miocene

**Occurrence:** This species occurs from the Upper Eocene (NP19) through Middle Miocene (NN4), but is far less abundant than the morphologically-similar *S. moriformis*. In Leg 154, the HO of *S. puniceus* is in Sample 925C-37-4, 30–32cm (15.498Ma, 0.020Ma error) and its HRO in Sample 925A-9-5, 130–131cm (16.517Ma, 0.020Ma error). In the GoM, the observed HO is coincident in age to the HRO in Leg 154.

### *Sphenolithus grandis* Haq & Berggren, 1978

Pl. 1, figs 27–30

1978 *Sphenolithus grandis* Haq & Berggren, p. 1192, pl. 3, figs. 17–20.

**Remarks:** The original authors distinguished *S. grandis* from *S. moriformis* by its large size (10–18$\mu$m) and elements disjoined throughout most of their length. Typically, it exhibits first order yellow to orange birefringence colors. Specimens as small as 8.5$\mu$m (the holotype) have been observed.

**Occurrence:** We have been unable to establish a reliable stratigraphic range for this species. In Leg 154, *S. grandis* occurs persistently in samples down into lower Zone NN6 and a single specimen was observed in upper Zone NN5. In the GoM, the HO was determined to be in middle Zone NN11. Perch-Nielsen (1985) showed a dashed range of Zones NN7-NN11 for this species.

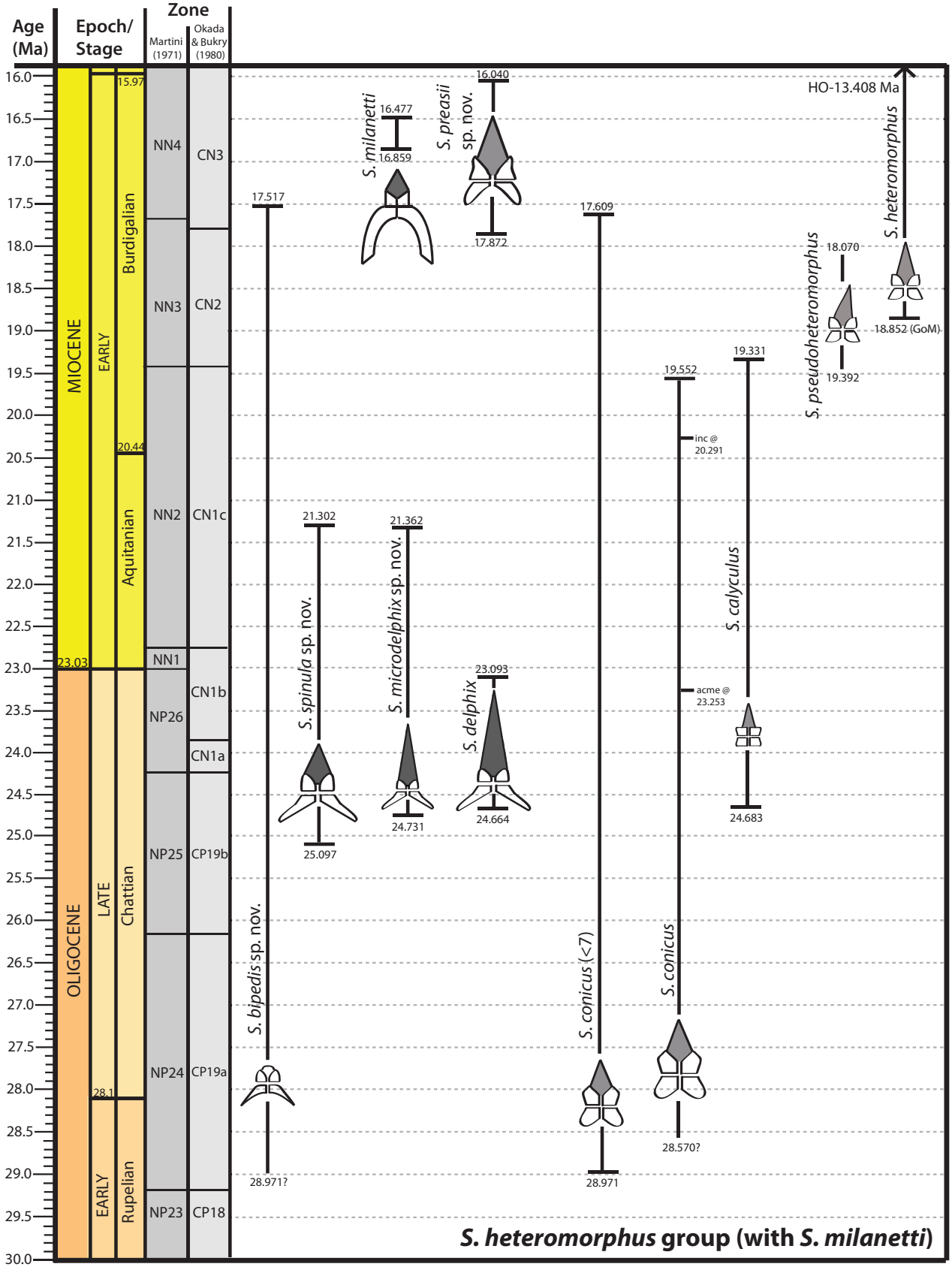


**Figure 5:** Range diagram of *Sphenolithus dissimilis* (2B), *S. heteromorphus* (2C), and *S. capricornutus* (3) morphologic groups

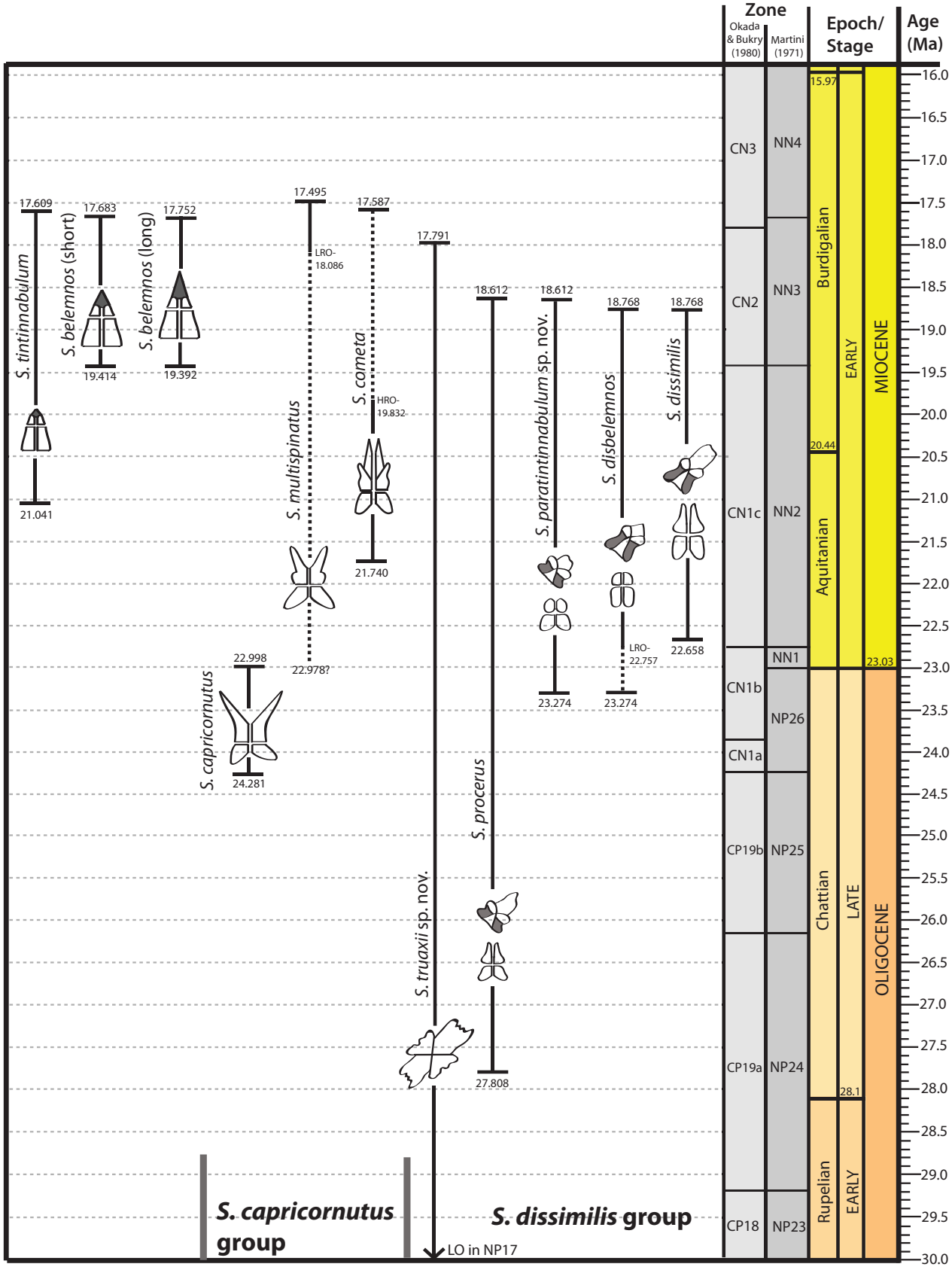
Zone
Okada & Bukry (1980)
Martini (1971)
Epoch/ Stage
Age (Ma)
CN3
CN2
CN1c
CN1b
CN1a
CP19b
CP19a
CP18
NN4
NN3
NN2
NN1
NP26
NP25
NP24
NP23
Burdigalian
Aquitanian
Chattian
Rupelian
EARLY
LATE
EARLY
MIOCENE
OLIGOCENE
15.97
20.44
23.03
28.1
16.0
16.5
17.0
17.5
18.0
18.5
19.0
19.5
20.0
20.5
21.0
21.5
22.0
22.5
23.0
23.5
24.0
24.5
25.0
25.5
26.0
26.5
27.0
27.5
28.0
28.5
29.0
29.5
30.0
S. tintinnabulum
17.609
21.041
S. belemnos (short)
17.683
19.414
S. belemnos (long)
17.752
19.392
S. multispinatus
17.495
LRO-18.086
22.978?
S. cometa
17.587
HRO-19.832
21.740
S. capricornutus
22.998
24.281
S. truaxii sp. nov.
17.791
LO in NP17
S. procerus
18.612
27.808
S. paratintinnabulum sp. nov.
18.612
23.274
S. disbelemnos
18.768
LRO-22.757
23.274
S. dissimilis
18.768
22.658
S. capricornutus group
S. dissimilis group

### 4.2A *Sphenolithus abies* group

This group is represented by conical sphenoliths with compound apical spines; the four species included are differentiated by their spine and proximal cycle morphologies (Table 3).

***Sphenolithus verensis* Backman, 1978**

Pl. 2, figs 1–4

1978 *Sphenolithus verensis* Backman, p. 111, pl. 2, figs. 4–6, 11, 12.

**Remarks:** *S. verensis* is retained for conical forms with compound apical spines and flared proximal elements.

**Occurrence:** We have been unable to establish a reliable stratigraphic range for *S. verensis* in the GoM. In Leg 154, its range has been established as Middle Miocene (NN5) through Middle Pliocene (NN16). The LO is placed in Sample 926A-29-2, 141–143cm (13.429Ma; 0.022Ma error) and the HO in Sample 926C-11H-4, 141–142cm (3.607Ma; 0.019Ma error).

***Sphenolithus abies* Deflandre *in* Deflandre & Fert, 1954**

Pl. 2, figs 5–10

1954 *Sphenolithus abies*, Deflandre *in* Deflandre & Fert, p. 41, pl. 10, figs. 1–4.

1967 *Sphenolithus moriformis* (Brönnimann & Stradner) Bramlette & Wilcoxon (*pro parte*), p. 124, pl. 3, figs. 5–6, *non* 1–4.

**Remarks:** Both of the specimens illustrated by light photographs by Deflandre (*in* Deflandre & Fert, 1954) are conical sphenoliths. Measurements of these two specimens and the three Upper Miocene specimens illustrated herein indicate that *S. abies* has a relatively shorter spine (height spine to base ratio: 0.26–0.70) and larger lateral element cycles (height upper to lower quadrant ratio measured in XPL: 0.82–0.99) than the older *Sphenolithus apoxis* n.sp.

**Occurrence:** In Leg 154, the LO of *S. abies* was placed within the Middle Miocene (NN5) in Sample 926A-29-6, 94–96cm (13.706Ma, 0.009Ma error); this event is not utilized in the GoM. Its HO represents the extinction of the genus in the Leg 154 research, dated at 3.510Ma (Table 1). However, the HO of the species in the GoM is immediately below those of *S. moriformis* and *S. neoabies* and believed to correspond to its HFO dated at 3.666Ma in the Leg 154 research (Table 1). The top acme appears coincident between the GoM and the Leg 154 research, observed in Sample 926C-12H-3, 70–71cm and dated at 3.909Ma (0.016Ma error) in the latter. The HO of larger specimens (> 6$\mu$m) is placed in Sample 926A-12H-3, 73–74cm and dated at 3.707Ma (0.020Ma error) in the Leg 154 research; this event is older in the GoM, correlated to the aforementioned top acme of the species in the Leg 154 research.

| SPECIES | GRP | SHAPE | PROXIMAL | OTHER DIAGNOSTIC FEATURES |
|---|---|---|---|---|
| *neoabies* | 1 | hemispherical | flared | flat base; younger than *bipedis* |
| *bipedis* | 1 | hemispherical | flared | arcuate base; older than *neoabies* |
| ***moriformis*** | 1 | hemispherical | | |
| *puniceus* | 1 | hemispherical | | blue-red birefringence colors |
| *grandis* | 1 | hemispherical | | large elements; > 8$\mu$m |
| *verensis* | 2A | conical | flared | |
| ***abies*** | 2A | conical | | shorter spine; younger than *apoxis* |
| *apoxis* | 2A | conical | | longer spine; older than *abies* |
| *pseudoradians* | 2A | conical | | spine: thick medial suture |

**Table 3:** *Sphenolithus* Identification Table (Groups 1 & 2A). Representative species for each group are bold-faced

***Sphenolithus apoxis* Bergen & de Kaenel, *sp. nov.***

Pl. 2, figs 11–20

1960 *Nannoturbella moriformis* Brönnimann & Stradner (*pro parte*), p. 368, figs. 14–15, *non* figs. 11–13, 16.

1971 *Sphenolithus dissimilis* Bukry & Percival (*pro parte*), p. 140, pl. 6, fig. 8, *non* figs. 7 & 9.

1997 *Sphenolithus dissimilis* Bukry & Percival 1971; Maiorano & Monechi, pl. 1, figs. 9–10.

**Derivation of name:** from Greek *apoxis*, meaning tapering off.

**Diagnosis:** Paleogene to Early Miocene conical sphenolith with a compound apical spine.

**Description:** Small to large, elongate conical sphenolith with a compound apical spine. The apical spine exhibits a sweeping extinction upon rotation; its termination is rounded. The three cited specimens and five illustrated herein have height to width ratios of 1.16–1.35; the relatively long apical spine (height spine to base ratio 0.75–0.91) and reduced lateral element cycles (height upper to lower quadrant ratio measured in XPL (0.30–0.75) are considered diagnostic). Size: 4.0–8.4$\mu$m (holotype: L = 6.0$\mu$m; W = 4.8$\mu$m).

**Remarks:** *Sphenolithus apoxis* has been illustrated under *S. moriformis* and *S. dissimilis*; the confusion with *S. dissimilis* is caused by a specimen illustrated (fig. 8) alongside the holotype (fig. 7) by Bukry and Percival (1971). *Sphenolithus dissimilis* has "shoulders", which are created by its cylindro-conical shape and the width differences between its base and spine. *Sphenolithus apoxis* has uniform taper (i.e. conical shape) and is not shouldered. *Sphenolithus apoxis* has a longer spine and reduced upper basal quadrants (lateral cycle elements) relative to *S. abies*. The two species do not co-occur and their stratigraphic ranges are separated by an estimated 3.7 million years in the Leg 154 research. *Sphenolithus apoxis* has been referred to as "*S.* cf. *procerus* (tapered)" in the BP GoM lexicon.

**Holotype:** Pl. 2, figs 15–16

**Type locality:** ODP Leg 154, Hole 929A, Ceará Rise, western equatorial Atlantic

**Type level:** Sample 35–3, 125–127cm (23.155Ma), Zone NP26, Upper Oligocene

**Occurrence:** This species ranges from the Lower Eocene (NP11) to Lower Miocene (NN4). In Leg 154, the HO of *S. apoxis* is dated at 17.347Ma and its HFO at 17.425Ma (Table 1). In the GoM, the observed HO is coincident in age to the HFO in Leg 154. The HO of larger variants (> 8$\mu$m) of *S. apoxis* may serve as a proxy for the HO of *S. pseudoradians* near the terminal Lower Oligocene and within Zone NP24; both extinctions have been dated at 28.092Ma in Leg 154 (see Table 1).

***Sphenolithus pseudoradians*** Bramlette & Wilcoxon, 1967

Pl. 2, figs 27–30

1967 *Sphenolithus pseudoradians* Bramlette & Wilcoxon, p. 126,. pl. 2, figs. 12–14.

**Remarks:** This species is easily distinguished by apparent thickening along the median axis of its apical spine.

**Occurrence:** Upper Eocene (NP18) to Lower Oligocene (NP24). The HO of *S. pseudoradians* has been dated at 28.092Ma in the Leg 154 research (Table 1) and is a marker in the GoM.

## 4.2B *Sphenolithus dissimilis* Group

Sphenoliths with bases that are either cylindrical or slightly conical (minimal taper distally) are placed within this group (Table 4). In specimens with high bases, the extinction lines cross and then parallel the lateral periphery (*S. dissimilis*, *S. disbelemnos*); if their bases are low, the extinction lines cross and continue to diverge (*S. procerus*, *S. paratintinnabulum*). All five species included in this group have compound apical spines. *Sphenolithus cometa* is closely related to members of this group (*S. procerus* and *S. dissimilis*), but is placed within the biconical Group 3 because of its narrowly divergent spine. Two new species are described, *Sphenolithus truaxii* and *Sphenolithus paratintinnabulum.*

***Sphenolithus truaxii*** **Bergen & de Kaenel, *sp. nov.***

Pl. 2, figs 21–26

**Derivation of name:** named in honor of GoM foraminifera specialist and native Louisianan, Stephen Truax III (retired BP).

**Diagnosis:** Cylindrical sphenolith whose lateral element cycle creates a distinct central bulge.

**Description:** Small to medium, elongate (length to width ratios 1.3–2.0), cylindrical sphenolith. The moderate to long spine is compound (sweeping extinction), but is less than or equal to the height of the base (height spine to base ratio 0.74–1.0). The lateral cycle (upper basal) is wider than both the spine and proximal cycle (lower basal); the height of the lateral cycle is less than or equal to the height of the proximal cycle. When oriented 45° to the polarizer, the linear extinction lines are oriented diagonally and their intersection orthogonal. Length: 4.6–6.8$\mu$m. (holotype: L = 6.8$\mu$m; W = 3.4$\mu$m).

**Remarks:** *Sphenolithus truaxii* is unique in being cylindrical and having a broad lateral cycle of elements, which gives the impression of a central bulge. When specimens are oriented 45° to the polarizer, the diagonal extinction cross appears linear and their intersection forms a 90° angle. *Sphenolithus truaxii* has been referred to as "*S. decussatus*" in the BP GoM lexicon.

**Holotype:** Pl. 2, figs 21–23

**Type locality:** ODP Leg 154, Hole 929A, Ceará Rise, western equatorial Atlantic

**Type level:** Sample 35-3, 125–127cm (23.155Ma), Zone NP26, Upper Oligocene

**Occurrence:** middle Eocene (NP17) through Lower Miocene (upper NN3). Its HO in Leg 154 was documented in Sample 928B-28-6, 40–41cm (17.791Ma, 0.021Ma error).

***Sphenolithus procerus*** **Maiorano & Monechi, 1997**

Pl. 3, figs 1–6

1997 *Sphenolithus procerus*, Maiorano & Monechi, p. 103, pl. 1, figs. 1–3.

1998 *Sphenolithus dissimilis* Bukry & Percival 1971; Young (*pro parte*), pl. 8.6, fig. 10, *non* fig. 9.

**Remarks:** *Sphenolithus procerus* is distinguished from *S. dissimilis* by its longer apical spine (length spine to base ratio > 1.0). Because of its shorter base, the extinction lines of *S. procerus* cross and are strongly divergent when specimens are oriented 45° to the polarizer. *S. procerus* also tends to have a broader spine than *S. dissimilis* (width of spine to base ratio > 0.50).

**Occurrence:** The HO of *S. procerus* is a GoM marker dated at 18.612Ma in the Leg 154 research (Table 1). The LO of *S. procerus* extends down near the base of the Upper Oligocene (Zone NP24) in GoM and Leg 154. In Leg 154, the LO is placed in Sample 926B-63X-6, 66–67cm (27.808Ma; 0.046Ma error).

| SPECIES | GRP | L/W | Up/Lo Quads | UPPER QUADS | LOWER QUADS | Spine/Base | Spine Length | OTHER DIAGNOSTIC FEATURE(S) |
|---|---|---|---|---|---|---|---|---|
| *truaxii* | 2B | > | = | bulged | | ≤ | medium | extinction "X" |
| *procerus* | 2B | > | = | | equant | > | long | extinction cross & diverge |
| ***dissimilis*** | 2B | > | < | | narrow | < | long | extinction cross & parallel |
| *disbelemnos* | 2B | > | < | | | << | v.short | height > width |
| *paratintinnabulum* | 2B | = | ≤ | | | << | v.short | base height = width |

**Table 4:** *Sphenolithus* Identification Table (Group 2B): cylindroconical. Representative species is bold-faced. L/W is a length/width ratio; Up/Lo Quads is a size ratio; Spine/Base is a length ratio

***Sphenolithus dissimilis*** Bukry & Percival, 1971
Pl. 3, figs 7–10

1971 *Sphenolithus dissimilis* Bukry & Percival (*pro parte*), p. 140–141, pl. 6, figs. 7, 9; *non* pl. 6, fig. 8.
*non* 1997 *Sphenolithus dissimilis* Bukry & Percival 1971; Maiorano & Monechi, pl. 1, figs. 9–10.
*non* 1998 *Sphenolithus dissimilis* Bukry & Percival 1971; Young, pl. 8.6, figs. 9–10.

**Remarks:** Bukry & Percival (1971) illustrated two XPL photomicrographs of *S. dissimilis*. The holotype has a "shouldered" appearance caused by the width difference between the spine and base, both of which are subcylindrical; the other specimen tapers uniformly and has a rounded distal termination. This other specimen (pl. 6, fig. 8) is considered here a different species (*S. apoxis*). Inclusion of these clearly conical forms in *S. dissimilis* is unwarranted.

*Sphenolithus dissimilis* is distinguished from *S. procerus* by its shorter apical spine (length spine to base ratio ≤ 1.0). Because of its higher base, the extinction lines of *S. dissimilis* cross and become nearly parallel when specimens are oriented 45° to the polarizer (Pl. 3, fig. 8). *Sphenolithus dissimilis* also tends to have a narrower spine than *S. procerus* (width spine to base ratio ≤ 0.50). Bukry & Percival (1971) stressed the difference in width between the three-part apical spine and wider base of *S. dissimilis*, in addition to the difference in birefringence between the lower (proximal cycle) and upper (lateral cycle) portions of the base. This contrast in optical birefringence, observed when specimens are oriented 45° to the polarizer, is most obvious in cylindroconical sphenoliths (Group 2B) and the *Sphenolithus belemnos* subgroup 2C1.

**Occurrence:** The HO of *S. dissimilis* and the HO of *S. disbelemnos* are markers for a Lower Miocene horizon in the GoM, both dated at 18.768Ma in Leg 154 research (Table 1). The LO of *S. dissimilis* is lowermost Miocene (NN2) in the GoM and Leg 154, dated at 22.658Ma (Table 1).

***Sphenolithus disbelemnos*** **Fornaciari & Rio, 1996**
Pl. 3, figs 11–28

1996 *Sphenolithus disbelemnos* Fornaciari & Rio, p. 28, pl. 2, figs. 7–10; pl. 3, 19–20; pl. 4, figs. 1–4.
1996 *Sphenolithus aubryae* de Kaenel & Villa, p.128, pl. 11, figs. 16–18.

**Remarks:** *Sphenolithus aubryae* and *S. disbelemnos* can be differentiated by size, using a practical length of 4$\mu$m based on their holotypes (Pl. 3, figs. 17–20). It would be expected that the smaller *S. disbelemnos* would have the longer stratigraphic range of the two species. However, the two species are considered synonymous herein because they were not differentiated in either the GoM or Leg 154 research. *Sphenolithus disbelemnos* has priority. *Sphenolithus disbelemnos* is more elongate (height to width ratios > 1.35) than *S. paratintinnabulum*.

**Occurrence:** The HO of *S. dissimilis* and the HO of *S. disbelemnos* are markers for a Lower Miocene horizon in the GoM, both dated at 18.768Ma in Leg 154 (Table 1). *Sphenolithus disbelemnos* has a distinct acme (HCO and LCO) in both GoM and Leg 154 within the lowermost Miocene (NN2), spanning approximately 220 kyr (Table 1). The LO of *S. disbelemnos* extends into the terminal Oligocene (NP26) in the GoM, the GSSP in northern Italy (9.4m below base Neogene), and Leg 154 (Sample 926B-51-3, 30–31cm; 23.274Ma; 0.019Ma error). In Leg 154, the LRO of the species within the basal Miocene (NN2) in Sample 928B-36-6, 100–102cm (22.757Ma; 0.020Ma error) is far more reliable than the LO of the species (single, isolated occurrence).

***Sphenolithus paratintinnabulum*** **Bergen & de Kaenel, *sp. nov.***
Pl. 3, figs 29–30; Pl. 4, figs 1–6

**Derivation of name:** from Greek *para*, meaning beside, near, or by, and from Latin *tintinnabulum*, meaning small bell.

**Diagnosis:** Equant cylindrical sphenolith with a very short compound spine.

**Description:** Small to medium, roughly cylindrical sphenolith. The height to width ratio of the base is equant to nearly equant (1.0–1.1). The compound conical spine is very short (spine to specimen length ratio 0.25–0.50). When oriented 45° to the polarizer, the lateral cycle displays a 1st order white birefringence, while the proximal cycle is faintly birefringent. At 0° in XPL, the upper quadrant (lateral cycle) appears shorter than the lower quadrant (proximal cycle). L = 2.2–3.6$\mu$m; W = 1.8–2.8$\mu$m (holotype: 2.8$\mu$m x 2.4$\mu$m). Length to width ratios of specimens 1.14–1.29. Ten specimens measured, including the four illustrated herein.

**Remarks:** *Sphenolithus paratintinnabulum* is distinguished from *S. tintinnabulum* by its roughly cylindrical shape, as the conical *S. tintinnabulum* is strongly tapered and triangular in lateral view.

**Holotype:** Pl. 4, figs 1–2

**Type locality:** ODP Leg 154, Hole 926B, Ceará Rise, western equatorial Atlantic

**Type level:** Sample 48-3, 30–32cm (22.208Ma), Zone NN2, Lower Miocene

**Occurrence:** The HO of *S. paratintinnabulum* is a useful Lower Miocene marker in the GoM, dated at 18.612Ma in Leg 154 (Table 1). The LO of *S. paratintinnabulum* extends into the terminal Oligocene (NP26) in the GoM and Leg 154, dated at 23.274Ma (Sample 926B-51-3, 30–31cm; 0.019Ma error).

## 4.2C *Sphenolithus heteromorphus* Group

Conical sphenoliths having apical spines that extinguish optically as a single unit (monocrystalline) are included in this group of ten species. Four subgroups are recognized on the morphology of the proximal element cycle

(i.e. lower quadrants) as they appear at 0º to the polarizer direction (Table 5). Taxa within each subgroup are distinguished by spine length and symmetry, as well as overall size.

### 4.2C.1 *Sphenolithus belemnos* subgroup (narrow proximal cycle)

The *S. belemnos* subgroup is distinguished by their narrow (height > width) lower quadrants of the proximal cycle, as they appear in XPL with specimens oriented N-S. In this orientation, the upper basal quadrants (lateral cycle) appear reduced relative to the lower basal quadrants (proximal cycle).

***Sphenolithus tintinnabulum*** Maiorano & Monechi, 1997

Pl. 4, figs 7–18

1997 *Sphenolithus tintinnabulum* Maiorano & Monechi, p. 104, pl. 1, figs. 4–6.

**Remarks:** Maiorano & Monechi (1997) diagnosed *S. tintinnabulum* as triangular in outline and having a very short apical spine. Their two XPL photomicrographs of a specimen show that the apical spine is monocrystalline. The two specimens in Maiorano & Monechi (1997) and three illustrated herein (Pl. 4, figs 7–9, 11–14) have apical spines whose length is less than 1/2 the total length of the specimen (holotype ~ 1/3). Such typical specimens of *S. tintinnabulum* are distinguished from *S. belemnos* by having shorter apical spines. Specimens identified as *S. tintinnabulum* with longer spines (Plate 4, figures 15–18), up to 2/3 the total length, are distinguished from *S. belemnos* by their flared proximal cycles and more delicate spines. *Sphenolithus tintinnabulum* differs from S. *paratintinnabulum* by its triangular outline.

**Occurrence:** The stratigraphic range of *S. tintinnabulum* in the Leg 154 material is from Sample 926B-44-5, 90–91cm (21.041Ma; 0.020Ma error) to Sample 928B-28-3, 145–146cm (17.609Ma; 0.022Ma error), encompassing Zones NN2 to NN4. The longer stemmed variants have been observed throughout Zone NN3 in Leg 154, but have not yet been fully investigated.

| SPECIES | SUB GRP | LOWER QUADS | SPINE LENGTH | OTHER DIAGNOSTIC FEATURE(S) |
|---|---|---|---|---|
| *tintinnabulum* | 2C1 | narrow | short | triangular base |
| ***belemnos*** | 2C1 | narrow | long | |
| ***calyculus*** | 2C2 | equant | long | equant quadrants |
| *conicus* | 2C2 | equant | medium | triangular outline |
| *preasii* | 2C2 | equant | medium | shouldered outline |
| *spinula* | 2C3 | flared | short | |
| *microdelphix* | 2C3 | flared | long | > 8μm |
| ***delphix*** | 2C3 | flared | long | ≤ 8μm |
| *pseudoheteromorphus* | 2C4 | broad | long | stem asymmetric |
| ***heteromorphus*** | 2C4 | broad | long | |

**Table 5:** *Sphenolithus* Identification Table (Group 2C): monocrystalline spines. Representative species for each subgrouping are bold-faced

***Sphenolithus belemnos*** Bramlette & Wilcoxon 1967

Pl. 4, figs 19–30

1967 *Sphenolithus belemnos* Bramlette & Wilcoxon, p. 118, pl. 2, figs. 1–3.

**Remarks:** Bramlette & Wilcoxon (1967) illustrated two specimens of *S. belemnos* in the same three light photomicrographs; they designated the upper specimen as the holotype. The holotype has a relatively longer apical spine (0.70 total specimen length) than the lower specimen (spine 0.60 total specimen length). More detailed examination of *S. belemnos* in the Leg 154 materials has shown stratigraphic potential in dividing this species into variants with relatively shorter (Pl. 4, figs 19–26) and longer (Pl. 4, figs 27–30) apical spines; this subdivision is currently placed where the apical spine is 2/3 of the total specimen length.

*Sphenolithus belemnos* is distinguished from typical *S. tintinnabulum* by their longer apical spines. In specimens with similar spine lengths, *S. tintinnabulum* is distinguished from *S. belemnos* by its flared base and more delicate apical spine.

**Occurrence:** The total range of *S. belemnos* defines Zone NN3, which is delineated in the Leg 154 data by variants with shorter apical spines. The LO of *S. belemnos* is utilized as a marker in the GoM and dated at 19.414Ma in Leg 154 (Table 1). The HO of the species in the GoM has been observed in less than 10% of wells and was previously interpreted as reworked; this event is dated at 17.683Ma (Table 1) and confirmed by two researchers in the Leg 154 materials. The HRO of *S. belemnos* in the GoM is a more reliable event, expressed as a top in more than 90% of wells examined; this event is dated at 17.831Ma in the Leg 154 research (Table 1).

### 4.2C.2 *Sphenolithus calyculus* subgroup (equant proximal cycle)

The *S. calyculus* subgroup is distinguished by the equant (height = width) lower quadrants of the proximal cycle. The three taxa in this group, roughly separated by the lengths of their monocrystalline apical spines, are better distinguished by their peripheral outlines and basal quadrant dimensions (Table 5). *Sphenolithus preasii* sp. nov. is described as new.

***Sphenolithus calyculus*** Bukry, 1985

Pl. 5, figs 1–6

1985 *Sphenolithus calyculus* Bukry, p. 600, pl. 1, figs. 13–19.

**Remarks:** We have measured eight specimens, including the holotype. Bukry (1985) mentioned that the height of upper and lower basal quadrants is the same when specimens are oriented at 0°; this has been confirmed and is considered diagnostic. Our measurements have demonstrated that the height of the base is equal to or slightly less than the width of the base (ratio 0.8–1.0). Bukry (1985) also described the spine being equal to or taller than the

base and this ratio varies from 1.0 to 2.5. The length of the species is revised to include specimens between 4.0 and 9.5$\mu$m in length, from the size of 5–9$\mu$m given by Bukry (1985).

**Occurrence:** The HO of *S. calyculus* is just above the base of Zone NN3, dated as 19.331Ma in Leg 154 (Table 1). Its LO is upper Oligocene (NP25) in both the GoM and Leg 154, where it is placed in Sample 926B-55-1, 80–81cm and dated at 24.683Ma (0.017Ma error).

***Sphenolithus conicus*** Bukry, 1971
Pl. 5, figs 7–18

1971 *Sphenolithus conicus* Bukry, p. 320, pl. 5, figs. 10–12.

**Remarks:** Bukry (1971a) described *S. conicus* as triangular in lateral view, suggesting it has uniform taper and a pointed apical spine. He distinguished it from *S. heteromorphus* by having a greater portion of base to spine (ratio > 1.0). *Sphenolithus conicus* and *S. preasii* sp. nov. have similar spine to base ratios, but *S. conicus* has a triangular outline (straight lateral periphery), convex indented proximal surface, and relatively taller upper quadrants (height upper to lower quadrant ratio > 0.80). *Sphenolithus apoxis* sp. nov. has a compound apical spine (sweeping extinction).

Bukry (1971a) restricted *S. conicus* to 7–12$\mu$m in length, but specimens as small as 4.4$\mu$m have been observed. It is much more difficult to discriminate smaller specimens of *S. conicus* because their common size and lower birefringence (1st order white) with other sphenoliths, especially in the high diversity assemblages near the end of its range in lower Zone NN4.

**Occurrence:** In Leg 154, *S. conicus* ranges from the upper Lower Oligocene (NP24) through Lower Miocene (NN4), reliably dated from 28.971Ma (Sample 925A-38R-3, 70–71cm; 0.041Ma error) to 17.609Ma (Sample 928B-28-3, 145–146cm; 0.022Ma error). The species also ranges down into the upper Lower Oligocene (NP 24) in the GoM, immediately above the HO of *S. pseudoradians*. The HO of *S. conicus* has long been utilized by BP as a GoM marker, but this event is associated with the top of the larger (> 7um) and more birefringent (1st order yellow to orange interference colors) specimens. The HO of large *S. conicus* in the GoM has been calibrated to its first downhole abundance increase in the Leg 154 research, dated at 20.291Ma (Table 1). The top acme of *S. conicus* is a deep-water GoM marker horizon in the terminal Oligocene (NP26) and is dated at 23.253Ma in the Leg 154 research (Table 1).

***Sphenolithus preasii* Bergen & de Kaenel, *sp. nov.***
Pl. 5, figs 19–30

**Derivation of name:** named in honor of geologist Patrick Preas of ALS-Ellington, Houston.

**Diagnosis:** Conical sphenolith with a monocrystalline apical spine, a "shouldered" lateral profile, and arcuate proximal surface.

**Description:** Medium to large, conical sphenolith. The monocrystalline apical spine is moderate to long (~ 1/2 to 3/4 the total length of the specimen), has a pointed to rounded apex, and becomes extinct when the specimen is aligned with the polarizing direction. In this orientation, the four basal quadrants each appear equant and the height of the upper quadrants is less than the height of the lower quadrants (0.67–0.76 ratio). In lateral profile, the proximal surface is concave and arcuate. The basal lateral periphery appears "bulged", giving the impression of shoulders when contrasted to the width of the spine at its juncture with the base (most evident at 45° in XPL). L = 5.6–10.0$\mu$m; W = 4.0–6.4$\mu$m (holotype: 9.8$\mu$m x 6.4$\mu$m).

**Remarks:** *Sphenolithus preasii* is somewhat transitional between *S. conicus* and *S. milanetti*. It differs from *S. conicus* by its "bulged" basal lateral periphery, arcuate proximal surface, and relatively lower upper quadrants (height upper to lower quadrant ratio < 0.8). *Sphenolithus milanetti* also has a "bulged" base, but its base is hemispherical and constructed of much larger elements. The basal upper quadrants (lateral cycle) of *S. milanetti* is much more reduced than in *S. preasii* (both height and width) relative to the size of their lower quadrants (proximal cycle). *Sphenolithus preasii* is also similar to *S. heteromorphus*, but the latter species is not shouldered (uniform taper), has a linearly indented proximal surface, and the height of its upper (lateral cycle) and lower (proximal cycle) quadrants are equal. The lower quadrant elements (proximal cycle) of *S. heteromorphus* appear broad (width > height), whereas those of *S. preasii* are equant. *Sphenolithus preasii* has been referred to as "*S. milanetti (elongate)*." in the BP GoM lexicon.

**Holotype:** Pl. 5, figs 28–30

**Type locality:** ODP Leg 154, Hole 925C, Ceará Rise, western equatorial Atlantic

**Type level:** Sample 38-6, 40–41cm (16.097Ma), Zone NN4, Lower Miocene

**Occurrence:** *Sphenolithus preasii* is rarely found in samples from the GoM. In Leg 154, this late Early Miocene species ranges from Sample 926B-35-3, 75–76cm (upper NN3) to Sample 925C-38-5, 95–96cm (middle NN4), which are dated from 17.872Ma (0.018Ma error) to 16.040Ma (0.022Ma error). The LO of larger specimens (>9$\mu$m) of *S. preasii* is in Sample 928B-28-4, 95–96cm in the Leg 154 research, dated at 17.672Ma (0.011Ma error).

## 4.2C.3 *Sphenolithus delphix* subgroup (flared proximal cycle)

The *S. delphix* subgroup is distinguished by its flared proximal cycle. Bukry (1973) referred to *S. delphix* as tri-radiate because of its long apical spine and laterally-extended proximal cycle. The three taxa in this group are distinguished by spine length and size (Table 5). Two new taxa are described in this subgroup, *S. spinula* and *S. microdelphix*.

***Sphenolithus spinula* Bergen & de Kaenel, *sp. nov.***

Pl. 6, figs 1–8

**Derivation of name:** from Latin *spinula*, diminutive of *spina*, meaning spine.

**Diagnosis:** Tri-radiate sphenolith with a short monocrystalline spine.

**Description:** Small to medium conical sphenolith. Specimens are triangular in profile, where length is equal to or slightly less than the width (ratio 0.85–1.0). The monocrystalline apical spine becomes extinct when specimens are aligned with the polarizer. The spine is short, approximately 1/2 of the total length of the specimen (spine to specimen length ration is 0.46–0.57), and has a pointed distal termination. At 0° to the polarizer, the upper basal quadrants appear shorter than the lower quadrants (1/2 to 3/4 height ratio). The proximal cycle elements flare laterally, where proximal cycle width approximately 1.5–2.0 times the width of the lateral cycle. The proximal surface is concave. L = 2.2–5.4$\mu$m; W = 2.6–5.4$\mu$m (holotype: 5.2$\mu$m x 5.2$\mu$m).

**Remarks:** This taxon differs from both *S. delphix and S. microdelphix* by its shorter apical spine. *Sphenolithus bipedis* sp. nov. and *S. neoabies* have flared proximal cycles, but are hemispherical forms with compound apical spines. *Sphenolithus spinula* sp. nov. is distinguished from *S. tintinnabulum* by its flared proximal elements characteristic of the *S. delphix* subgroup. It tends to be larger and broader (length < width) than *S. tintinnabulum*, but there is significant overlap in the size and dimensions of these two species. *Sphenolithus spinula* has been referred to as "*S. delphix* (stumpy)" in the BP GoM lexicon.

**Holotype:** Pl. 6, figs 1–3

**Type locality:** ODP Leg 154, Hole 926B, Ceará Rise, western equatorial Atlantic

**Type level:** Sample 50-5, 140–142cm (23.072Ma), Zone NP26, upper Oligocene

**Occurrence:** *Sphenolithus spinula* ranges from the Upper Oligocene (NP25) to lowermost Miocene (NN2) in the GoM and Leg 154. It is dated in the Leg 154 research from 25.097Ma (Sample 925A-26-5, 125–126cm; 0.027Ma error) to 21.302Ma (Sample 926B-45-4, 45–46cm; 0.028Ma error).

***Sphenolithus microdelphix* Bergen & de Kaenel, *sp. nov.***

Pl. 6, figs 9–20

**Derivation of name:** from Greek *mikros*, meaning small and *delphix*, meaning tripod.

**Diagnosis:** small to medium, tri-radiate sphenolith with a long monocrystalline spine.

**Description:** Small to medium conical sphenolith. Specimens are tri-radiate in profile, where length is equal to or greater than the width (ratio 1.0–1.75). The monocrystalline apical spine is greater than 2/3 of the total length of the specimen. Its becomes extinct when specimens are aligned with the polarizer. In this orientation, the upper basal quadrants (lateral cycle) appear equal to or less than the height of the lower quadrants (proximal cycle). The base of the proximal cycle elements flare laterally and proximally; their width is 1.5–2.0 times the width of the lateral cycle. The proximal surface is concave. Specimen length is less than 8$\mu$m. Length of ten measured specimens: 2.4–6.4$\mu$m; width measured specimens: 2.4–5.2$\mu$m (holotype: 5.2$\mu$m x 5.0$\mu$m).

**Remarks:** *Sphenolithus microdelphix* differs from *S. delphix* by being smaller and from *S. spinula* by its longer apical spine. This taxon has been referred to as "*S.* cf. *delphix* (small)" in the BP GoM lexicon.

**Holotype:** Pl. 6, figs 11–13

**Type locality:** ODP Leg 154, Hole 929A, Ceará Rise, western equatorial Atlantic

**Type level:** Sample 35-3, 125–27cm (23.155Ma), Zone NP26, upper Oligocene

**Occurrence:** *Sphenolithus microdelphix* ranges from Upper Oligocene (NP25) through lowermost Miocene (NN2). The HO of *S. microdelphix* is a marker in the GoM, dated at 21.362Ma in Leg 154 (Table 1). The LO is dated at 24.731Ma (928B-41-5, 140–141cm; 0.028Ma error) in Leg 154.

***Sphenolithus delphix* Bukry, 1973**

Pl. 6, figs 21–25

1973 *Sphenolithus delphix* Bukry, p. 679, pl. 3, figs. 19–22.

**Remarks:** Bukry (1973) gave the length of *S. delphix* as 8–12$\mu$m and that criterion is followed herein. It is distinguished from *S. microdelphix* sp. nov. by its size and from *S. spinula* sp. nov. by its size and longer spine.

**Occurrence:** *Sphenolithus delphix* is restricted to the uppermost Oligocene (upper NP25-NP26). Its stratigraphic range is coeval between the GoM and Leg 154. The HO of *S. delphix* is a GoM marker and dated at 23.093Ma in Leg 154 (Table 1); its HO is positioned 3.5 meters below the base Neogene in the GSSP section in northern Italy. In Leg 154, the LO was seen in Sample 926B-55-1, 25–26cm, dated at 24.664Ma (0.019Ma error).

### 4.2C.4 *Sphenolithus heteromorphus* subgroup (broad proximal cycle)

The *S. heteromorphus* subgroup is distinguished by its broad lower quadrants (proximal cycle). Only two taxa are considered in this subgroup, *S. heteromorphus* and *S. pseudoheteromorphus* (Table 5).

***Sphenolithus pseudoheteromorphus* Fornaciari & Agnini, 2009**

Pl. 7, figs 1–5

2009 *Sphenolithus pseudoheteromorphus* Fornaciari & Agnini, p. 97, pl. 1, figs. 1–16; pl. 2, figs. 1–5, 9, 13.

**Remarks:** This species is well illustrated in Fornaciari & Agnini (2009). The asymmetry of its monocrystalline apical spine is considered diagnostic.

**Occurrence:** Fornaciari & Agnini (2009) reported the range of this species within NN2. We have observed this species in the GoM and Leg 154, but its stratigraphic range is not well constrained. In Leg 154, *S. pseudoheteromorphus* has been observed intermittently in lower Zone NN3 from Sample 926C-39-5, 110–112cm (19.392Ma; 0.022Ma error) to Sample 926B-35-6, 140–141cm (18.070Ma; 0.017Ma error).

### *Sphenolithus heteromorphus* Deflandre, 1953

Pl. 7, figs 6–13

1953 *Sphenolithus heteromorphus* Deflandre, p. 1786, p. 1, figs. 1–2.

**Remarks:** Deflandre (1953) published a light photomicrograph of a single specimen. This holotype and the four specimens illustrated herein share the following properties: (1) the apical spine is higher than the base: (2) the height of the upper and lower quadrants (lateral and proximal cycles) appear equal when specimens are aligned with the polarizer; and (3) the height to width ratio of the proximal element cycle is less than 1/2. Length is highly variable; specimens as small as 4.0$\mu$m have been observed.

**Occurrence:** The HO of *S. heteromorphus* marks the top of Zone NN5 (13.408Ma). Four *S. heteromorphus* events are utilized in the GoM Basin by BP, all of which have ages established in Leg 154 (Table 1). Three of these events appear coeval between the GoM and Leg 154. The 17.791Ma age for the LO of *S. heteromorphus* established in Leg 154 (Table 1) is younger than that observed in the GoM. In many deep-water GoM wells, the LO of *S. heteromorphus* has been associated with the HO of *Discoaster saundersii*, dated at 18.852Ma in our Leg 154 research (Sample 926B-38-3, 15–17cm; 0.020Ma error).

## 4.3 *Sphenolithus capricornutus* group

The *S. capricornutus* group is characterized by their flared (i.e., distally divergent) apical spines (Table 6), resulting in a biconical shape.

### *Sphenolithus multispinatus* Maiorano & Monechi, 1997

Pl. 7, figs 14–17

1997 *Sphenolithus multispinatus* Maiorano & Monechi, p. 104, pl. 1, figs. 14–16.

**Remarks:** Six specimens were measured, including the two original specimens of Maiorano & Monechi (1997). The angle between the divergent apical spines ranges from 42–56° and specimen length between 3–6$\mu$m. Maiorano & Monechi (1997) stated a length of "about 6–7$\mu$m" for the species. *Sphenolithus multispinatus* has a more divergent spine than *S. cometa*, but less divergent spine than *S. capricornutus*. Damaged specimens of *S. multispinatus* with single or no spines can be confused with *S. calyculus* - these two species have similar bases.

**Occurrence:** Maiorano & Monechi (1997) gave a range of upper Zone NN3 to lower Zone NN4 for *S. multispinatus* at DSDP Site 563 in the North Atlantic. Its HO is in lower Zone NN4 for both the GoM and Leg 154, observed in Sample 928B-28-2, 80–82cm and dated at 17.495Ma (0.031Ma error). The LRO in Leg 154 is in upper Zone NN3 in Sample 926B-35-7, 32–33cm and dated at 18.086Ma (0.026Ma error). The species occurs very sporadically in Leg 154 samples down into Zone NN2 (Sample 926C-40-6, 60–62cm; 19.792Ma). Single specimens were also observed in Sample 926B-44-3, 85–86cm (20.950Ma; NN2) and Sample 926B-50-4, 40–41cm (22.978Ma; NN1).

### *Sphenolithus cometa* de Kaenel & Villa, 1996

Pl. 7, figs 18–25

1996 *Sphenolithus cometa* de Kaenel & Villa, p. 128, pl. 11, figs. 22–24.

**Remarks:** For *S. cometa*, the narrow divergence of its branched spine (~ 10–36°) distinguishes it from *S. capricornutus* and *S. multispinatus*. *Sphenolithus cometa* can be more difficult to distinguish from *S. dissimilis* and *S. procerus*, which are other "shouldered" forms with long, sub-cylindrical, compound apical spines, though the distal spine of those two species is not branched. L = 3.6–7.0$\mu$m.

**Occurrence:** The HRO of *S. cometa* has been used in the GoM, for which an age of 19.832Ma has been established in Leg 154 (Table 1). In Leg 154, it ranges from middle Zone NN2 to lower Zone NN4. The stratigraphic range of the species is very reliable in Leg 154, where it is dated from 21.740Ma (926B-46-7, 5–6cm; 0.025Ma error) to 17.587Ma (Sample 928B-28-3, 110–112cm; 0.024Ma error).

### *Sphenolithus capricornutus* Bukry & Percival, 1971

Pl. 7, figs 26–30

| SPECIES | GRP | L/W | Up/Lo Quads | LOWER QUADS | Spine/Base | Spine Length | OTHER DIAGNOSTIC FEATURE(S) |
|---|---|---|---|---|---|---|---|
| *cometa* | 3 | > | ≤ | variable | > | long | narrow divergence |
| *multispinatus* | 3 | > | ≤ | variable | = | long | wide divergence |
| ***capricornutus*** | 3 | ≥ | ≤ | broad | > | medium | wide divergence |
| *milanetti* | 4 | > | << | hemisph. | ≤ | medium | monocrystalline spine |
| *avis* | 4 | = | - | hemisph. | << | short | duocrystalline spine |
| ***umbrellus*** | 4 | = | - | hemisph. | - | none | no spine |

**Table 6:** *Sphenolithus* Identification Table (Groups 3 & 4): biconical and sphaeroconical. Representative species for each group are bold-faced. L/W is a length/width ratio; Up/Lo Quads is a size ratio; Spine/Base is a length ratio

1971 *Sphenolithus capricornutus* Bukry & Percival, p. 140, pl. 6, figs. 4–6.

**Remarks:** Seven specimens were measured, including the two original specimens of Bukry & Percival (1971). The angle between the divergent apical spines ranges from 54–76°. Bukry & Percival (1971) gave a size range of 6–10$\mu$m, but specimens as small as 4.8$\mu$m in length have been observed. *Sphenolithus capricornutus* has a more divergent spine than *S. cometa* and *S. multispinatus*.

**Occurrence:** The HO of *S. capricornutus* approximates the top of the Oligocene in the GoM, Leg 154 and the Italian GSSP. It actually ranges just into the basal Neogene in the GSSP section in northern Italy (0.4m above base Neogene) and in Leg 154 (22.998Ma; Table 1). The LO in Leg 154 is upper Oligocene (NP25), where it is dated at 24.281Ma (Table 1). In the Italian GSSP, it is present in the bottom sample studied (26.9 meters below the base of the Neogene).

## 4.4 *Sphenolithus umbrellus* group

The *S. umbrellus* group has a sphaeroconical shape. The three species included herein have hemispherical bases constructed of very large, strongly arcuate elements. Species are distinguished by their apical spines (Table 6).

### *Sphenolithus milanetti* Maiorano & Monechi, 1998

Pl. 8, figs 1–9

1998 *Sphenolithus milanetti* Maiorano & Monechi, p. 249, pl. 2, figs. 30–31.

2016 *Sphenolithus pospichalii* Jiang, Wang, Varol, da Gama & Blaj, p. 61, pl. 1, figs. 1–8.

**Remarks:** *Sphenolithus milanetti* is distinguished by its hemispherical proximal cycle constructed of large elements, short monocrystalline spine, and reduced lateral cycle elements. Maiorano & Monechi (1998) mentioned that the proximal cycle elements (lower basal quadrants) are about twice as large as the lateral cycle elements (upper basal quadrants); our measurements of six specimens confirm this observation both in the height (0.29–0.47) and width (0.43–0.58) ratios of the small upper to larger lower quadrants. The spine is approximately half the length of the specimen, but may be reduced to 1/3 the total length (Plate 8, figs. 7–9). Maiorano & Monechi (1998) gave a size range of 6–10$\mu$m for the species.

This species differs from *S. umbrellus* by having a spine and from *S. avis* by having lateral elements and a monocrystalline spine. Both *S. umbrellus* and *S. avis* are Oligocene species. *Sphenolithus milanetti* may actually be more closely related to other Miocene sphenoliths with monocrystalline spines, all of which have conical shapes. In fact, *S. preasii* sp. nov. seems the most likely ancestor to *S. milanetti* (Figure 5).

*Sphenolithus pospichalii* is considered here a junior synonym, as its dimension ratios are nearly identical to *S. milanetti*; both species are reported restricted to NN4 and given nearly identical size ranges. Specimens of *S. pospichalii* illustrated by Jiang *et al*. (2016) are better preserved than the holotype of *S. milanetti*.

**Occurrence:** *Sphenolithus milanetti* has been rare in deep-water GoM samples. It is restricted to Zone NN4 in Leg 154, where it ranges from Sample 928A-26-2, 85–86cm (16.859Ma; 0.015Ma error) to Sample 925A-9-5, 50–51cm (16.477Ma; 0.021Ma error); its HRO occurs in Sample 925A-9-6, 105–106cm (16.579Ma; 0.020Ma error).

### *Sphenolithus avis* Aljahdali, Wise, Bergen & Pospichal, 2015

Pl. 8, figs 10–24

2015 *Sphenolithus avis* Aljahdali, Wise, Bergen & Pospichal, p. 193, pl. 1, figs. 1–5; pl. 2, figs. 1–6.

**Remarks:** The diagnosis of *S. avis* by Aljahdali *et al*. (2015) stressed its "short tapered apical spine and wide flaring proximal basal elements that at the end taper proximally". All light and electron photomicrographs of the species show a short tapered distal projection composed of two elements. The lanceolate sphenoliths also possess duocrystalline spines and are Paleogene, as is *S. avis* (Figure 6). The short apical spine of *S. avis* is 1/3 to 2/3 the length of the specimen (versus less than 1/2). Length to width ratio includes specimens slightly taller than wide (ratio 0.9–1.2). Size range: 3.3–6.5$\mu$m.

The proximal elements of *S. avis* are very large and form a hemispherical shape, features which its shares with *S. umbrellus* and *S. milanetti;* however, *S. umbrellus* has no distal projection. *Sphenolithus milanetti* is a late Early Miocene species with a monocrystalline, spine and prominent lateral elements. *Sphenolithus avis* is also smaller and has a lower length to width ratio than *S. milanetti*. This taxon has been referred to as "*S. proboscis*" and "*S. truaxii*" in the BP GoM lexicon.

**Occurrence:** The HRO of *S. avis* in Leg 154 (26.627Ma; Table 1) is coincident with the HO established in deep-water GoM wells over the past decade. The HO of *S. avis* has since been placed within Zone NP25 in Leg 154 research and dated at 24.408Ma; the LO in the GoM and Leg 154 is within Zone NP23 and tentatively dated at 30.512Ma (Table1).

### *Sphenolithus umbrellus* (Bukry, 1971) Aubry & Knüttel *in* Knüttel, 1986

Pl. 8, figs 25–30

1971 *Catinaster*? *umbrellus* Bukry, p. 50, pl. 3, figs. 10–13.

1986 *Sphenolithus umbrellus* (Bukry, 1971) Aubry & Knüttel, *in* Knüttel, p. 279, pl. 5, figs. 1, 2, 5–10.

**Remarks:** Bukry (1971b) mentioned *S. umbrellus* has no knob or ornamentation and its simple construction of a single cycle of elements (no spine or lateral elements) makes it unique among the genus *Sphenolithus*. Bukry (1971b) gave a size range of 8–12$\mu$m for the species; measured specimens from the two citations and our work range from

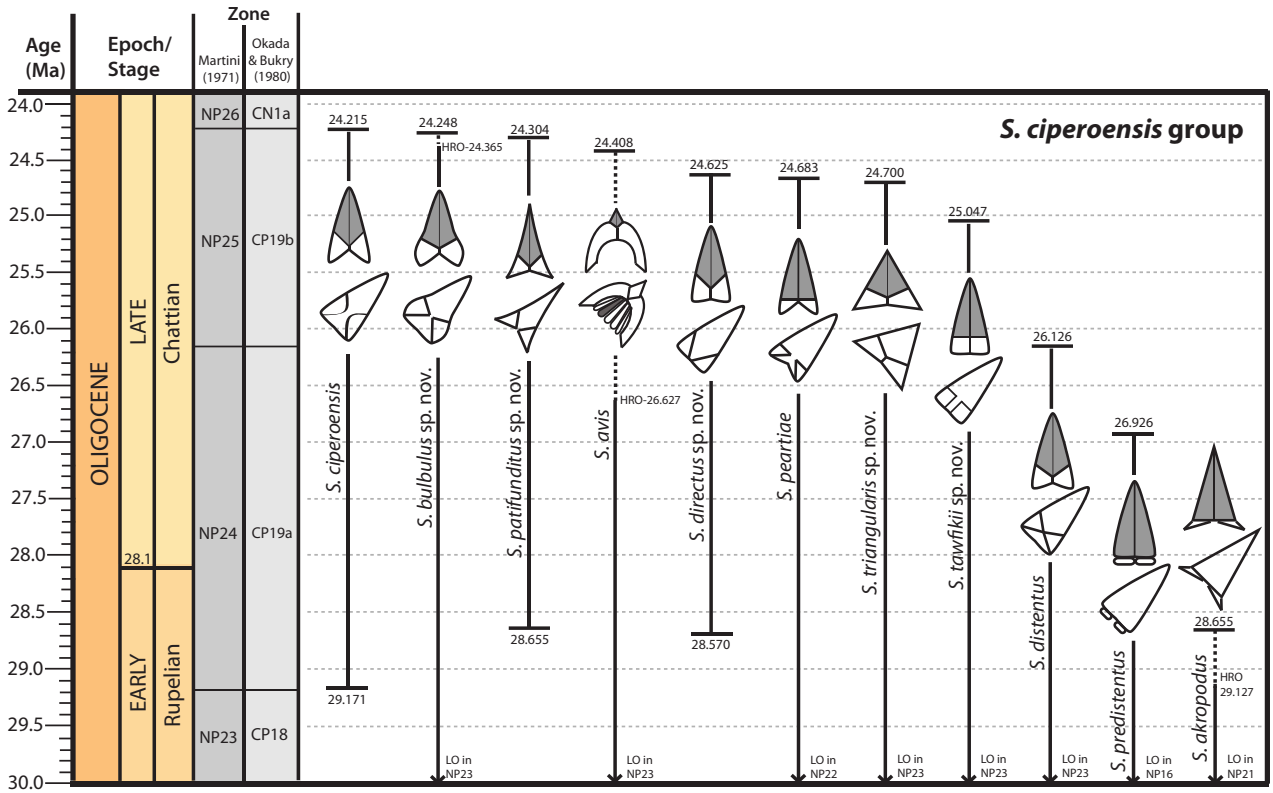


**Figure 6:** Range diagram of *Sphenolithus ciperoensis* (5) morphologic group

4.4–8.0$\mu$m high by 4.8–10.35$\mu$m wide. Height is equal to or less than its width (ratio 0.65–1.00) and its shape in top view is circular to broadly elliptical. It is possible that *S. umbrellus* may have originated from *S. avis* by developing a higher proximal cycle and the complete loss of an apical spine.

**Occurrence:** The HO of *S. umbrellus* has been observed in the Upper Oligocene in six deep-water GoM wells, where it has been associated with the HO of *S. ciperoensis* (top Zone NP25). This is roughly coincident to the HRO of S. umbrellus in the Leg 154 research, dated at 24.233Ma (Sample 926B-53X-5, 110–11cm; 0.018Ma error). The HO was observed stratigraphically higher near the top of Zone NN1 in Sample 928B-37-1, 10–11cm and dated at 22.819Ma (0.021Ma error). The LO in Leg 154 is in Zone NP24, but is unreliable and placed in Sample 928B-48X-6, 3–4cm (27.890Ma; 0.040Ma error).

## 4.5 *Sphenolithus ciperoensis* group

These lanceolate sphenoliths appear smooth in XPL because their spines are duocrystalline and their basal elements are small. It is assumed all taxa within this group have delicate and long branched spines, whose branches are not usually preserved. For this reason, length is measured on complete specimens from the proximal surface to the point of maximum constriction below the flared distal branch. Within this lanceolate group, taxonomic separation is primarily based on the extinction pattern when specimens are oriented 45° degrees to the polarizer. The subgroupings are further divided based on extinction angle or orientation (Table 7). Extinction angles can differ significantly between sides of the same specimen. *Sphenolithus triangularis* sp. nov. is distinguished solely on its equidimensional outline in lateral view. Half the species included in this group are new or emended. Drawings representing the extinction patterns and lateral outlines of the twelve taxa in the *S. ciperoensis* group are shown in Figure 7 and with their ranges (along with *S. avis*) in Figure 6.

***Sphenolithus ciperoensis*** Bramlette & Wilcoxon, 1967
Pl. 9, figs 1–8

1967 *Sphenolithus ciperoensis* Bramlette & Wilcoxon, p. 120, pl. 2, figs. 15–20.

**Remarks:** The length of the holotype for *S. ciperoensis* is about 6.3$\mu$m. Cross-polarized light micrographs of this specimen show extinction lines that touch at 0° to the polarizer, but are separated and form obtuse extinction angles when oriented at 45°. The lateral periphery of *S. ciperoensis* is straight, from which distinguishes it from two new species described herein, *S. patifunditus* (concave peripheral surface on proximal cycle) and *S. bulbulus* (convex peripheral surface on proximal cycle).

**Occurrence:** The LO and HO of *S. ciperoensis* define the base of Zone NP24 (CP19a) and top Zone NP25 (CP19b), respectively. The stratigraphic ranges of two sizes of *S. ciperoensis* are well-constrained in both the GoM and Leg 154 (Table 1). Specimens greater than

| SPECIES | LENGTH/ WIDTH | LATERAL PERIPHERY | PROXIMAL CYCLE | EXTINCTION LINES | | OTHER DIAGNOSTIC FEATURE(S) |
|---|---|---|---|---|---|---|
| | | | | Angle | Orientation | |
| ***ciperoensis*** | > | linear | | obtuse | diagonal | |
| *patifunditus* | > | concave | flared | obtuse | diagonal | |
| *tawfikii* | > | linear | | = 90 | axial | aligned main axes |
| *bulbulus* | > | convex | bulged | ~90 | diagonal | ext. lines separate at 45° |
| *distentus* | > | linear-convex | | acute | diagonal | ext. lines touch at 45° |
| *akropodus* | > | concave | flared | acute | variable | |
| *peartiae* | > | linear | | acute | variable | |
| *predistentus* | > | linear | feet | 0 | horizontal | smaller (≤ 9µm) |
| *celsus* | > | linear | feet | 0 | horizontal | larger (> 9µm) |
| *tribulosus* | > | linear | feet | 0 | horizontal | serrate spine |
| *directus* | > | linear | | 0 | diagonal | |
| *triangularis* | = | linear | | | diagonal | equidimensional |

**Table 7:** *Sphenolithus* Identification Table (Group 5): lanceolate. Representative species is bold-faced

6$\mu$m, akin to the size of the holotype, have a shorter stratigraphic range than smaller specimens. The base of Zone NP24 is delineated on the LO of *S. ciperoensis* - confirmed by two researchers in our Leg 154 materials – and dated at 29.171Ma. Specimens at the base of its range are very small, less than 3$\mu$m. Older appearances for *S. ciperoensis* reported in published literature are assumed to include broader taxonomic concepts, such as *S. bulbulus* sp. nov. (eg. Raffi *et al*., 2016). The top of Zone NP25 represents the extinction of lanceolate sphenoliths and is dated herein at 24.215Ma (Table 1). The first downhole increase in *S. ciperoensis* has stratigraphic utility in the GoM and has been tied to the HCO of the species in the Leg 154 research dated at 24.456Ma (Table 1).

### *Sphenolithus patifunditus* Bergen & de Kaenel, *sp. nov.*

Pl. 9, figs 9–16

**Derivation of name:** from Latin *pateo*, meaning lie open and *funditus*, meaning entirely, totally, completely.

**Diagnosis:** An elongate lanceolate sphenolith with a flared base and concave peripheral surfaces along its length.

**Description:** Small, elongate, conical sphenolith. In lateral view, specimens appear smooth in XPL, as is typical of lanceolate sphenoliths. At 0° to the polarizer, the spine is faintly birefringent and bisected by a longitudinal suture; the base is brightly birefringent (1st order white) and its two extinction lines touch along the longitudinal axis. At 45° to the polarizer, the entire specimen exhibits a 1st order white birefringence. The paired extinction lines remain separate in this orientation, their individual extinction angles are obtuse or nearly obtuse (80–120°), and the extinction lines are oriented diagonally. The base is flared with a concave peripheral surface. L = 4.4–4.9$\mu$m; W = 2.8–3.0$\mu$m (holotype 4.8$\mu$m x 2.8$\mu$m).

**Remarks:** *Sphenolithus patifunditus* is distinguished from all other lanceolate sphenoliths by its flared base and concave peripheral surfaces, along with its obtuse extinction angles. *Sphenolithus ciperoensis* has straight lateral peripheries. *Sphenolithus akropodus* is an Early Oligocene species with a flared base, but its extinction angles are acute. *Sphenolithus patifunditus* has been referred to as "*S. ciperoensis* (flared)" in the BP GoM lexicon.

**Holotype:** Pl. 9, figs 11–12

**Type locality:** ODP Leg 149, Hole 899B, eastern equatorial Atlantic

**Type level:** Sample 9-6, 15–16cm, Zone NP25, Upper Oligocene

**Occurrence:** The HO of *S. patifunditus* is much more reliable than the LO in both the GoM and Leg 154. The HO is in Sample 926B-54X-1, 60–61cm dated at 24.304Ma (0.023Ma error) in Leg 154, with specimens observed in 8 of 10 samples at the top of its range. The LO was observed in Sample 928B-50X-2, 5–6cm and dated at 28.655Ma (0.028Ma error) in Leg 154 by two researchers, but observed in only 2 of 10 samples at the base of its range. The LO was calibrated in only two deep-water GoM wells.

### *Sphenolithus tawfikii* Bergen & de Kaenel, *sp. nov.*

Pl. 9, figs 17–20

**Derivation of name:** Named in honor of Egyptian nannofossil biostratigrapher Essam Tawfik.

**Diagnosis:** A lanceolate sphenolith whose paired extinction lines are oriented parallel to the main axes and have orthogonal extinction angles.

**Description:** Medium-sized, elongate, conical sphenolith. In lateral view, specimens appear smooth in XPL, as is typical of lanceolate sphenoliths. At 0° to the polarizer, the spine is faintly birefringent and the extinction lines of the brightly birefringent (1st order white) blocky basal elements touch or nearly touch. At 45° to the polarizer, the entire specimen exhibits a 1st order white birefringence. The paired extinction lines remain separate in this orientation, their individual extinction angles are orthogonal, and the extinction lines are oriented parallel to the main axes of the sphenolith. The spine may have a

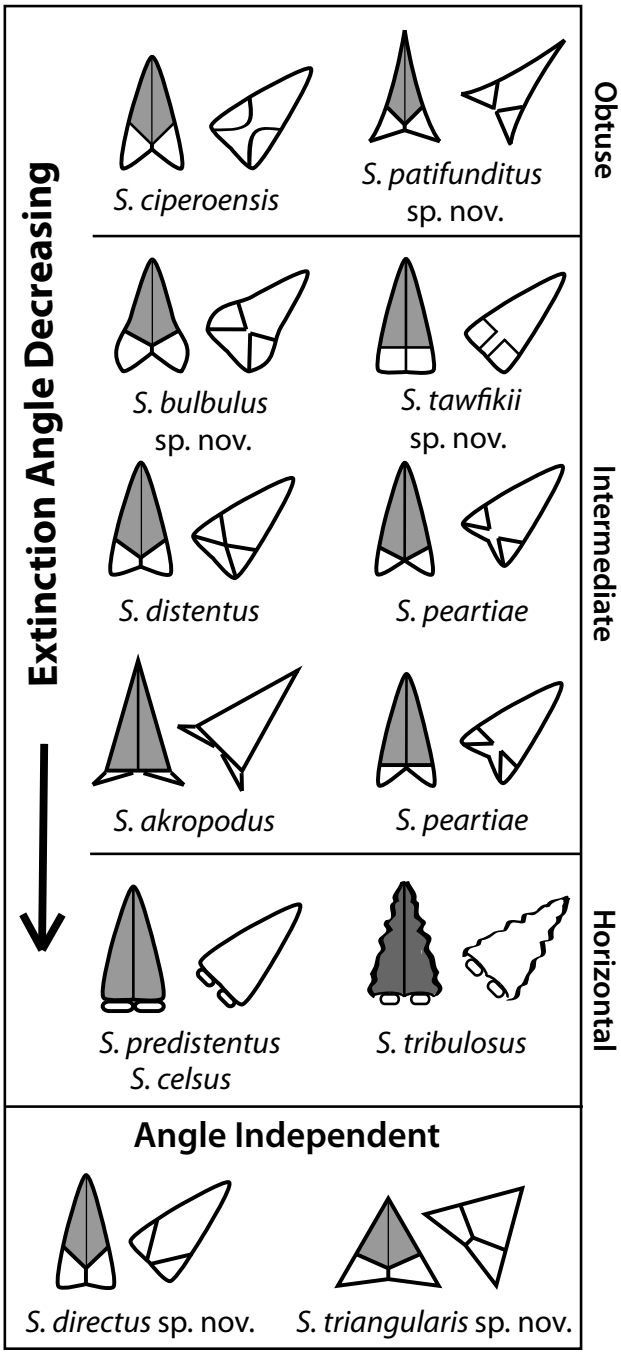


**Figure 7:** Schematics of *Sphenolithus* taxa within morphologic Group 5 (*S. ciperoensis*). Taxa are subdivided based on their extinction angle

longitudinal suture and be branched. L = 5.6–6.0$\mu$m; W = 3.2–3.6$\mu$m (two specimens).

**Remarks:** The orthogonal extinction angles, combined with the alignment of the extinction lines with the main axes of the sphenolith, are diagnostic for *S. tawfikii*. *Sphenolithus tawfikii* has been referred to as "*S. cathetus*" in the BP GoM lexicon.

**Holotype:** Pl. 9, figs 19–20

**Type locality:** DSDP Leg 101, Hole 628A, western Atlantic

**Type level:** Sample 23-3, 80–81cm, Zone NP25, Upper Oligocene

**Occurrence:** The HO of *S. tawfikii* is used as a marker in the GoM, where it is paired with the HO of *Helicosphaera bramlettei*. The HO of *S. tawfikii* is coeval in Leg 154, where it is dated at 25.047Ma (Table 1). Its LO has been documented in the middle Lower Oligocene in the GoM (mid NP23), but below the reach of our Leg 154 research (30.679Ma).

### *Sphenolithus directus* Bergen & de Kaenel, *sp. nov.*

Plate 9, figures 21–24

**Derivation of name:** from Latin *directus*, meaning straight, direct, set in order.

**Diagnosis:** A lanceolate sphenolith with two linear to slightly curved extinction lines, each extending from the lateral to proximal peripheries.

**Description:** Small to medium, elongate, conical sphenolith. In lateral view, specimens appear smooth in XPL, as is typical of lanceolate sphenoliths. At 0° to the polarizer, the spine is faintly birefringent and the extinction lines of the brightly birefringent (1st order white) basal elements touch. At 45° to the polarizer, the entire specimen exhibits a 1st order white birefringence. The paired extinction lines remain separate in this orientation, each extending diagonally from the lower lateral periphery to middle proximal periphery, forming a high angle to the horizontal. The extinction lines are linear to somewhat curved (concave toward the peripheries). L = 3.2–5.2$\mu$m; W = 2.4–2.8$\mu$m (two specimens).

**Remarks:** The diagonal extinction lines of *S. directus* are linear to slightly curving – unique among the lanceolate sphenoliths. *S. directus* has been referred to as "*S.* aff. *ciperoensis*" in the BP GoM lexicon.

**Holotype:** Pl. 9, figs 23–24

**Type locality:** DSDP Leg 101, Hole 628A, western Atlantic

**Type level:** Sample 23-5, 80–81cm, Zone NP25, Upper Oligocene

**Occurrence:** The HO of *S. directus* was first established within Zone NP25 in the GoM; this event was placed in Sample 926B-54-6, 115–116cm in Leg 154 and dated at 24.625Ma (0.032Ma error). The LO was observed in Sample 928B-50X-1, 15–16cm and dated at 28.570Ma (0.042Ma error).

### *Sphenolithus bulbulus* Bergen & de Kaenel, *sp. nov.*

Pl. 9, figs 25–30; Pl. 10, figs 1–6

**Derivation of name:** from Latin *bulbulus* (diminutive), meaning a swelling.

**Diagnosis:** An elongate lanceolate sphenolith with a bulged, convex base (proximal cycle periphery) whose extinction lines remain separate at 45° and have orthogonal extinction angles.

**Description:** Small to medium, elongate, lanceolate sphenolith. In lateral view, specimens appear smooth in XPL, as is typical of lanceolate sphenoliths. At 0° to

the polarizer, the spine is faintly birefringent to dark and bisected by a longitudinal suture; the base is brightly birefringent (1st order white) and its two extinction lines touch or nearly touch along the longitudinal axis. At 45° to the polarizer, the entire specimen exhibits a 1st order white birefringence. The paired extinction lines remain separate in this orientation. The diagonal extinction lines are oriented symmetric about the horizontal axis and extinction angles vary around orthogonal (80–110°). The base has a convex lateral periphery (bulged). The proximal surface is often concave. L = 4.4–6.4$\mu$m; W = 2.4–4.0$\mu$m; base height 1.6–2.8$\mu$m; height spine to base ratio 1.3–2.8 (14 specimens).

**Remarks:** *Sphenolithus bulbulus* is distinguished by its bulged base and diagonal extinction lines, which at 45° remain separate and form roughly orthogonal extinction angles. In *S. distentus*, the extinction lines touch at 45° to the polarizer, extinction angles are lower, and the lateral periphery is typically straight. *Sphenolithus ciperoensis* has a straight lateral periphery and higher extinction angles. *Sphenolithus bulbulus* has been referred to as "*S. distentus* var." in the BP GoM lexicon.

**Holotype:** Pl. 10, figs 3–4

**Type locality:** ODP Leg 149, Hole 900A, eastern equatorial Atlantic

**Type level:** Sample 49-3, 113–114cm, Zone NP24, Upper Oligocene

**Occurrence:** The HO of *S. bulbulus* is a GoM marker, which is coeval to its HRO in Leg 154 (24.365Ma); *S. bulbulus* ranges higher in the Mediterranean (Italy and Egypt) and Leg 154 (Table 1). The LO is in lower Zone NP23, below the reach of our Leg 154 research.

***Sphenolithus distentus*** (Martini, 1965) Bramlette & Wilcoxon, 1967, **Bergen & de Kaenel, emend.**

Pl. 10, figs 7–14

1965 *Furcatolithus distentus* Martini, p. 407, pl. 35, figs. 7–9.

1967 *Sphenolithus distentus* (Martini, 1965) Bramlette & Wilcoxon; p. 122, pl. 1, fig. 5, pl. 2, figs. 4–5.

1971 *Sphenolithus distentus* (Martini, 1965) Bramlette & Wilcoxon; Roth, Franz & Wise, p. 1103, pl. 2, figs. 1–9; pl. 3, figs. 1–2; text-fig. 5.

1971 *Sphenolithus distentus* (Martini, 1965) Bramlette & Wilcoxon; Martini, pl. 3, figs. 11–12.

**Emended description:** An elongate, lanceolate sphenolith with diagonal extinction lines symmetric about the horizontal axis; the extinction lines touch at the median (no white birefringence between their apices) when specimens are oriented 45° to the polarizer. Extinction angles in this orientation are moderately acute to orthogonal (35–90°) and the entire specimen brightly (1st order white) birefringent. At 0°, the spine is weakly birefringent and the two bright basal element touch at the median. The lateral outline is straight, but rare specimens may have a convex basal periphery. The height of the base is about 0.8–1.6$\mu$m. The long conical apical spine may branch.

**Remarks:** The holotype designated by Martini (1965) is incomplete, only a brightly birefringent apical spine with long branches typical of the entire lanceolate group. This is further complicated by an original description focused on the long branches and mention of a Miocene age for this specimen. Bramlette & Wilcoxon (1967) recombined the species into *Sphenolithus*, realizing its stratigraphic utility in the Oligocene and correcting the age of the type material. Although they did not emend the species, Bramlette & Wilcoxon (1967) illustrated the first light photomicrographs of a complete specimen and described a depressed base composed of 10–12 spines attached to a slightly convex base on a large apical spine. Roth *et al*. (1971) published 11 electron photomicrographs of *S. distentus*, mentioning a proximal shield composed of 10–14 elements. Of more practical help is their sketch of *S. distentus* (text-fig. 5) showing diagonal extinction lines symmetric across the horizontal axis and touching at the median axis, with an acute extinction angle (40°). Martini (1971) used the HO of *S. distentus* to define the top of NP24 in his Cenozoic zonation, which he accompanied with two light photomicrographs. Common features to all the aforementioned light photomicrographs of complete specimens, as well as the sketch, are diagonal extinction lines symmetrical about the horizontal that touch at the median. The light photomicrograph of Bramlette & Wilcoxon (1967) differs in having higher extinction angles and a base with a convex basal periphery. The four specimens in Bramlette & Wilcoxon (1967) and Martini (1971) have bases between 1.0–1.5$\mu$m high, as opposed to the 2–5$\mu$m mentioned by Roth *et al*. (1970).

*Sphenolithus distentus* is distinguished by its diagonal extinction lines which touch at 45° to the polarizer. *Sphenolithus bulbulus* sp. nov. has a higher base, higher extinction angles (80–110°), and diagonal extinction lines that remain separate at 45°. *Sphenolithus peartiae* and *S. distentus* have similar extinction angles and base heights, but the extinction lines of *S. peartiae* remain separate at 45° and their orientation may be asymmetric about the horizontal axis. *Sphenolithus predistentus* has a shorter base (< 0.75$\mu$m) and horizontal extinction line marking the base of the spine.

**Occurrence:** The HO of *S. distentus* defines the base of Zone NP25 (CP19b) and the LO the base of Zone CP18, which subdivides Zone NP23. Both events are GoM markers. The HO of *S. distentus* has been dated in Leg 154 at 26.126Ma (Table 1), whereas the LO in lower Zone NP23 is below the reach of our Leg 154 research.

***Sphenolithus triangularis*** **Bergen & de Kaenel, *sp. nov.***

Pl. 10, figs 15–24

**Derivation of name:** from Latin *triangulus*, meaning having three angles.

**Diagnosis:** A triangular lanceolate sphenolith whose height is equal to or slightly less than its width.

**Description:** Small to medium, roughly equidimensional, triangular sphenolith. Height of specimen is equal to or slightly less than the width (ratio 0.8–1.0). In lateral view, specimens appear smooth in XPL, as is typical of lanceolate sphenoliths. At 0° to the polarizer, the spine is faintly birefringent to dark and the extinction lines of the brightly birefringent (1st order white) basal elements touch. At 45° to the polarizer, the entire specimen exhibits a 1st order white birefringence. The paired extinction lines remain separate in this orientation, their individual extinction angles variable (50–140°), even on the same specimen. The extinction lines are oriented diagonally. The short spine may have a longitudinal suture. The lateral peripheries are linear and the proximal surface normally indented. L = 2.0–4.4$\mu$m; W = 2.4–5.6$\mu$m (eight specimens).

**Remarks:** The equidimensional outline of *S. triangularis* distinguishes it from all other lanceolate sphenoliths. *Sphenolithus avis* is the same size with nearly identical height to width dimensions and also has a short spine, but has a convex basal periphery and large proximal elements. The straight lateral periphery of *S. triangularis* distinguishes it from *S. avis* in poorly preserved assemblages.

**Holotype:** Pl. 10, figs 17–18

**Type locality**: Cipero coast, north end, Locality 10 of Bolli (1957), south Trinidad

**Type level:** Sample JS20, *Globorotalia opima opima* Zone, Lower Oligocene, Zone NP24

**Occurrence:** The HO of *S. triangularis* is used as marker in the GoM, where it is paired with the HO of *S. ciperoensis* (> 6$\mu$m). This event is also within Zone NP25 in Leg 154, dated at 24.700Ma (Table 1). In the GoM, the LO of the species falls in lower Zone NP23, below the Leg 154 research (30.679Ma).

***Sphenolithus akropodus*** de Kaenel & Villa, 1996

Pl. 10, figs 25–30; Pl. 11, figs 1–4

1996 *Sphenolithus akropodus* de Kaenel & Villa, p. 127, pl. 11, figs. 1, 2, 4–11.

**Remarks:** *Sphenolithus akropodus* was thoroughly documented by de Kaenel & Villa (1996), including two specimens transferred between the SEM and LM. Its proximal elements extend just outside the lateral periphery of the spine, which is diagnostic. Only *S. patifunditus* sp. nov. shares this proximal lateral extension among the lanceolate sphenoliths, but its entire lateral periphery is concave. In *S. akropodus*, the base of the apical spine is convex and sometimes bulged. De Kaenel & Villa (1996) gave the length of the species as 7–9$\mu$m, but we have observed specimens as small as 5.8$\mu$m long. The extinction angle varies from moderately acute to orthogonal (35–90°) and its orientation relative to the horizontal is variable. *Sphenolithus peartiae* shares these two extinction properties, but lacks the proximal lateral extinction. For *S. akropodus*, longer specimens tend to have higher extinction angles and length to width ratios, which may prove useful to the eventual recognition of a new taxon.

**Occurrence:** There is stratigraphic merit in separating the species into two size categories at 8$\mu$m length, as their extinctions have utility in both the GoM and Leg 154, bracketing the NP23/NP24 boundary (Table 1). The HRO of *S. akropodus* is also a GoM marker, approximating the top of Zone NP23 (Table 1). The LO of *S. akropodus* is in lower Zone NP21 in the GoM.

***Sphenolithus peartiae*** Bown & Dunkley Jones, 2012, **Bergen & de Kaenel, emend.**

Pl. 11, figs 5–14

2012 *Sphenolithus peartiae* Bown & Dunkley Jones, p. 34, pl. 11, figs. 39–44.

**Emended description:** small to medium, elongate, conical sphenolith. In lateral view, specimens appear smooth in XPL, as is typical of lanceolate sphenoliths. At 0° to the polarizer, the spine is faintly birefringent to dark and the extinction lines of the brightly birefringent (1st order white), wedged-shaped basal elements touch or nearly touch along the longitudinal axis. At 45° to the polarizer, the entire specimen exhibits a 1st order white birefringence. The paired extinction lines remain separate in this orientation, their individual extinction angles are moderately acute (40–75°), and their orientation relative to the horizontal is symmetric or asymmetric (projecting proximally). The long spine can display a longitudinal suture (best seen at 0°) and its termination may be branched. The lateral peripheries are linear and the proximal surface normally indented. L = 3.6–8.2$\mu$m; W = 2.8–4.8$\mu$m. Height of base: 0.8–2.2$\mu$m; height spine to base ratio 2.2–6.0 (27 specimens).

**Remarks:** Bown & Dunkley Jones (2012) described *S. peartiae* with a "low base that meets the spine along horizontal or near horizontal sutures, but when 45° to polarizing direction a birefringent structure passes between the basal 'feet'." This description includes the holotype of *S. predistentus* and is not a means to differentiate the two species. A lot of the variation in the extinction lines of the *S. distentus* - *S. predistentus* plexus is taken up by *S. peartiae*. *Sphenolithus predistentus* is reserved herein for specimens with horizontal extinction lines and rounded to narrow wedge-shaped (extinction angle < 20°) "feet" and lower bases (< 0.75$\mu$m). *Sphenolithus distentus* is reserved herein for specimens with diagonal extinction lines symmetric to the horizontal, which touch when specimens are oriented 45° to the polarizer. *Sphenolithus akropodus* displays similar extinction angles and orientations to *S. peartiae*, but differs in the lateral extension of its base. In *S. bulbulus* sp. nov., the base is bulged (convex basal periphery). *Sphenolithus peartiae* has been referred to as "*S. predistentus* var." and "*S. parviquetrus*" in the BP GoM lexicon.

**Occurrence:** There is stratigraphic utility in separating *S. peartiae* into two size categories at 7$\mu$m length,

as their extinctions fall on either side of the NP24/NP25 boundary in both the GoM and Leg 154 (Table 1). The LO of *S. peartiae* is in mid Zone NP22 in the GoM.

***Sphenolithus predistentus*** Bramlette & Wilcoxon, 1967

Pl. 11, figs 15–20

1967 *Sphenolithus predistentus* Bramlette & Wilcoxon, p. 126, pl. 1, fig. 6; pl. 2, figs. 10–11.

**Remarks:** The holotype of *S. predistentus* is illustrated by two light photomicrographs of a specimen in XPL, oriented at 0° and 45°. This specimen has an apical spine that tapers to a point and is divided by a longitudinal suture. More importantly, Bramlette & Wilcoxon (1967) mention that the base of the apical spine is flat, which on the holotype results in a horizontal extinction line separating the spine from two rounded "feet". These two feet are separated so that the extinction lines extend downward (proximally) between them to form a point. In some specimens, the basal feet are wedge-shaped (Plate 11, figures 17–18). The extinction lines are either horizontal at the base of the spine or have an extinction angle less than 20°. Height of base: 0.4–0.74$\mu$m; height spine to base ratio: 7.3–9.9 (two cited specimens and four herein). The horizontal extinction at the base of the spine and rounded basal "feet" characterize *S. predistentus*, along with the larger *S. celsus* (i.e., specimens of *S. predistentus* > 9$\mu$m) and the serrate *S. tribulosus*. *Sphenolithus predistentus* grades into *S. peartiae* (Pl. 11, fig. 16), which displays a higher extinction angle (specimens oriented at 45°) and has a higher base – resulting in lower spine to base ratios.

**Occurrence:** The HO of *S. predistentus* has long been utilized as a marker in the GoM by all three BP heritage companies, historically the next significant "top" below that of *S. distentus* (top NP24). This exceptionally reliable event has been dated at 26.926Ma in our Leg 154 research (Table 1). The LO of S. predistentus is in Middle Eocene (NP16) in the GoM.

***Sphenolithus tribulosus*** Roth, 1970

Pl. 11, figs 21–24

1970 *Sphenolithus tribulosus* Roth, p. 870, pl. 14, figs. 5, 7–8.

**Remarks:** The serrate apical spine of *S. tribulosus* is diagnostic and is clear on the holotype (electron photomicrograph). Its extinction pattern groups it with *S. celsus* and *S. predistentus*, which do not have serrate apical spines. The light photomicrographs of the specimen illustrated by Roth (1970) show the entire specimen a bright 1st order white birefringence at 45° to the polarizer with a horizontal proximal surface below which are two separate, rounded "feet". At 0°, the spine of this specimen is weakly birefringent and divided by a longitudinal suture. Roth (1970) stated the length of the holotype as 6.5$\mu$m, but it is only 5.1$\mu$m long up to the base of the bifurcation.

**Occurrence:** *S. tribulosus* has not been differentiated from *S. predistentus* in the GoM. In Leg 154, the HO has been placed in Sample 925A-41R-CC, 12–13cm within Zone NP23 and dated at 29.886Ma (0.036Ma error). Perch-Nielsen (1985) showed the LO of this species in NP21.

***Sphenolithus celsus*** Haq, 1971

Pl. 11, figs 25–30

1971 *Sphenolithus celsus* Haq, p. 121, pl. 1, figs. 1–5; pl. 5, fig. 4.

**Remarks:** Haq (1971) described a sphenolith with a large stem protruding from a short base; the holotype (an electron photomicrograph) also has a branched apical spine characteristic of the lanceolate group. The light photomicrographs of the two specimens illustrated by Haq (1971) show a horizontal proximal surface below which are two separate, rounded "feet" (i.e. small proximal cycle elements) and a spine divided longitudinally by a suture. Haq (1971) gave a size range of 10–18$\mu$m for the species, but our measurements of his three specimens indicate ≥ 9.0$\mu$m as a better definition (without branching). Specimens less than 9.0$\mu$m are identified as *S. predistentus*. Length to width ratio of cited specimens (four) and those herein (two) are 2.5–3.4.

**Occurrence:** *S. celsus* ranges from the Upper Eocene (NP19) to Lower Oligocene (near base of NP23) in deep-water GoM wells.

**Genus *Ilselithina*** Roth, 1970

***Ilselithina fusa*** Roth, 1970

Pl. 6, figs 26–30

1970 *Ilselithina fusa* Roth, p. 856, pl. 7, figs. 2–3.

**Remarks:** Roth (1970) mentioned the lower number of distal (6–10) and proximal shield (10–15) elements, as well as antenna-like distal elements that are normally damaged. The very small sizes of the holotype (2.4$\mu$m) and paratype (3.0$\mu$m) seem anomalous. Specimens observed range from 3.2$\mu$m to 5.2$\mu$m. *Ilselithina fusa* has a low number of proximal shield elements (i.e. large), a feature it shares with the sphaeroconical sphenoliths (*S. umbrellus* group). It differs from that group of sphenoliths by having an open central area and a flared distal cycle of elements.

**Occurrence:** The range of *I. fusa* in the GoM is lowermost Oligocene (lower NP21) through lower Miocene (upper NN2). The HO is a GoM marker; in Leg 154, this event was placed in Sample 926B-40-6, 50–52cm and dated at 19.712Ma (0.024Ma error).

## 5. Depositories

The slides and samples are stored in the micropaleontological collections of the Natural History Museum in Basel (NMB) in Switzerland. Also curated at the NMB are the samples of the foraminifera collections of H.M. Bolli (1957), which have been used to describe some of the new species herein.

Type material from DSDP and ODP cores are also stored at the Bremen repository (Germany) and at College Station repository (USA). ODP sample request numbers for Leg 154 are: 18687A (2003), 18687B (2005), 20484A (2005), 20484B (2006), 22364B (2011), 22433A (2011). Leg 154 nannofossil abundance data will be archived in the web database, PANGAEA (www.pangaea.de).

## Acknowledgements

We are grateful to many people in BP GoM Exploration for their support and encouragement over the years. We thank Graham "Pinky" Vinson and Liz Jolley for permission to publish this manuscript. Special thanks are extended to Jim Newell, whose work for two of the BP heritage companies contributed greatly to this work. Our gratitude is extended to Drs. David Watkins and Richard Howe for reviewing this manuscript.

## References

Aljahdali, M, Wise, S.W., Bergen J. & Pospichal, J.J. 2015. A new biostratigraphically significant Late Oligocene *Sphenolithus* species from the equatorial region. *Micropaleontology*, **61**(3): 193–197.

Aubry, M.-P. 2014. Cenozoic coccolithophores: Discoasterales (CC-B). *Atlas of Micropaleontology Series*. Micropaleontology Press, New York: 532pp.

Backman, J. 1978. Late Miocene–Early Pliocene nannofossil biochronology and biogeography in the Vera Basin, SE Spain. *Acta University Stockholm Contributions in Geology*, **32**(2): 93–114.

Bergen, J.A., Truax III, S., de Kaenel, E., Blair, S., Browning, E., Lundquist, J., Boesiger, T., Bolivar, M., & Clark, K. *in prep*. BP Gulf of Mexico Neogene Astronomically-tuned Time Scale. *GSA Bulletin.*

Bergen, J., Truax, S., Kaenel, E., de, Boesiger, T., Gamber, J., Lundquist, J. & Febo, L. 2009. Microfossil definition of the Oligocene-Miocene boundary and its application in the Gulf of Mexico. Geologic Problem Solving with Microfossils II: Abstracts with Programs: 21–22.

Blair, S., Bergen, J., de Kaenel, E., Browning, E. & Boesiger, T. 2017. Upper Miocene – Lower Pliocene taxonomy and stratigraphy in the circum North Atlantic Basin: radiation and extinction of Amauroliths, Ceratoliths, and the *Discoaster quinqueramus* lineage. *Journal of Nannoplankton Research*, **37**(2/3): 113–144.

Bolli, H.M. 1957. Planktonic Foraminifera from the Oligocene-Miocene Cipero and Lengua Formations of Trinidad, B.W.I. *Bulletin of the American Museum of Natural History*, **215**: 97–123.

Bramlette, M.N. & Riedel, W.R. 1954. Stratigraphic value of Discoasters and some other microfossils related to Recent coccolithophores. *Journal of Paleontology*, **28**(4): 385–403.

Bramlette, M.N. & Wilcoxon, J.A. 1967. Middle Tertiary calcareous nannoplankton of the Cipero Section, Trinidad, W.I. *Tulane Studies in Geology and Paleontology*, **5**(3): 93–132.

Brönnimann, P. & Stradner, H. 1960. Die Foraminiferen- und Discoasteridenzonen von Kuba und ihre interkontinentale Korrelation. *Erdoel-Z.*, **76**(10): 364–269.

Bown, P.R. & Dunkley Jones, T. 2012. Calcareous nannofossils from the Paleogene equatorial Pacific (IODP Expedition 320 Sites U1331–1334). *Journal of Nannoplankton Research*, **32**(2): 3–51.

Bukry, D. 1971a. Cenozoic calcareous nannofossils from the Pacific Ocean. *San Diego Society of Natural History Transactions*, **16**(14): 303–327.

Bukry, D. 1971b. Discoaster evolutionary trends. *Micropaleontology*, **17**(1): 43–52.

Bukry, D. 1973. Coccolith stratigraphy, eastern equatorial Pacific, Leg 16 Deep Sea Drilling Project. *Initial Reports of the DSDP*, **16**: 653–711.

Bukry, D. 1985. Mid-Atlantic ridge coccolith and silicoflagellate biostratigraphy, Deep Sea Drilling Sites 558 and 563. *Initial Reports of the DSDP*, **82**: 591–603.

Bukry, D. & Bramlette M.N. 1969. Some new and stratigraphically useful calcareous nannofossils of the Cenozoic. *Tulane Studies in Geology and Paleontology*, **7**: 131–142.

Bukry, D. & Percival, S.F. 1971. New Tertiary calcareous nannofossils. *Tulane Studies in Geology and Paleontology*, **8**: 123–146.

Deflandre, G. 1953. Hétérogénéité intrinsèque et pluralité des éléments dans les coccolithes actuels et fossils. *Comptes rendus Académie des sciences*, Paris, **237**: 1785–1787.

Deflandre, G. & Fert, C. 1954. Observations sur les coccolithophorides actuels et fossils en microscopie ordinaire et electronique. *Annales de Paléontologie*, **40**: 115–176.

De Kaenel, E. & Bergen, J. 2008. Middle Miocene lineages in the calcareous nannofossil genus Discoaster. *In*: INA 12 abstracts, Lyon, France, September, 2008: 47.

De Kaenel, E., Bergen, J., Blair, S., Boesiger, T. & Browning, E. 2017. Uppermost Oligocene to Middle Miocene Discoaster and Catinaster taxonomy and stratigraphy in the circum North Atlantic. *Journal of Nannoplankton Research*, **37**(2/3), 215–244.

De Kaenel, E. & Villa, G. 1996. Oligocene–Miocene calcareous nannofossil biostratigraphy and paleoecology from the Iberia Abyssal Plain. *Proceedings of the ODP, Scientific Results*, **149**: 79–145.

De Kaenel, E. & Villa, G. 2010. Nannofossil definition of the Oligocene/Miocene boundary at Lemme-Carrosio (Italy). *In:* INA 13 abstracts, Yamagata, Japan September 2010: 33.

Fornaciari, E. & Agnini, C. 2009. Taxonomic note: Sphenolithus pseudoheteromorphus, a new Miocene calcareous nannofossil species from the equatorial Indian Ocean. *Journal of Nannoplankton Research*, **30**(2): 97–101.

Fornaciari, E. & Rio, D. 1996. Latest Oligocene to early middle Miocene quantitative calcareous nannofossil biostratigraphy in the Mediterranean region. *Micropaleontology*, **42**(1): 1–36.

Gartner, S. Jr. 1967. Calcareous nannofossils from Neogene of Trinidad, Jamaica, and Gulf of Mexico. *The University of Kansas Paleontological Contributions*, **29**: 1–7.

Haq, B.U. 1971. Paleogene Calcareous nannoflora, Part III, Oligocene of Syria. *Stockholm Contributions in Geology*, **25**(3): 99–127.

Haq, B.U. & Berggren, W.A. 1978. Late Neogene calcareous plankton biochronology of the Rio Grande Rise (South Atlantic Ocean). *Journal of Paleontology*, **52**(6): 1167–1194.

Hay, W.W., Mohler, H.P., Roth, P.H., Schmidt, R.R. & Boudreaux, J.E. 1967. Calcareous nannoplankton zonation of the Cenozoic of the Gulf Coast and Caribbean-Antillean area, and transoceanic correlation. *In:* Symposium on the geological history of the Gulf of Mexico, antillean Caribbean region. *Transactions of the Gulf Coast Association of Geological Societies*, **17**: 428–480.

Jiang, S., Wang, Y., Varol, O., da Gama, R.O.B.P. & Blaj, T. 2016. A new early Miocene Sphenolithus species from the South China Sea. *Journal of Nannoplankton Research*, **36**(1): 61–63.

Knüttel, S. 1986. Calcareous nannofossil biostratigraphy of the central East Pacific Rise, Deep Sea Drilling Project Leg 92: evidence for downslope transport of sediments. *Initial Reports of the DSDP*, **92**: 255–290.

Martini, E. 1965. Mid-Tertiary calcareous nannoplankton from Pacific deep-sea cores. *Proceedings of the 17th Symposium of the Colston Research Society*, 393–411.

Martini, E. 1971. Standard Tertiary and Quaternary calcareous nannoplankton zonation. *In:* A. Farinacci (Ed.). *Proceedings of the Second Planktonic Conference Roma 1970*. Edizioni Tecnoscienza, Rome, **2**: 739–785.

Martini, E. & Bramlette, M.N. 1963. Calcareous nannoplankton from the experimental Mohole drilling. *Journal of Paleontology*, **37**(4): 845–856.

Maiorano, P. & Monechi, S. 1997. New Early Miocene species of *Sphenolithus* Deflandre, 1952 from the North Atlantic Ocean. *Journal of Nannoplankton Research*, **19**(2): 103–107.

Maiorano, P. & Monechi, S. 1998. Revised correlations of Early and Middle Miocene nannofossil events and magnetostratigraphy from DSDP Site 563 (North Atlantic Ocean). *Marine Micropaleontology*, **35**: 235–255.

Okada, H. & Bukry, D. 1980. Supplementary modification and introduction of code numbers to the low-latitude coccolith biostratigraphic zonation (Bukry, 1973; 1975). *Marine Micropaleontology*, **5**: 321–325.

Perch-Nielsen, K. 1985. Cenozoic calcareous nannofossils. *In:* H.M. Bolli, J.B. Saunders & K. Perch-Nielsen (Eds). *Plankton Stratigraphy*. Cambridge University Press, Cambridge: 427–554.

Raffi, I., Agnini, C., Backman, J., Catanzariti, R., & Pälike, H. 2016. A Cenozoic calcareous nannofossil biozonation from low and middle latitudes: A synthesis. *Journal of Nannoplankton Research*, **36**(2): 121–132.

Roth, P.H., 1970. Oligocene calcareous nannoplankton biostratigraphy. *Eclogae Geologicae Helvetiae* **63**(3): 799–881.

Roth, P.H., Franz, H.E. & Wise, S.W. 1971. Morphological study of selected members of the Genus Sphenolithus Deflandre (Incertae Sedis, Tertiary). *In:* A. Farinacci (Ed.). *Proceedings of the Second Planktonic Conference Roma 1970*. Edizioni Tecnoscienza, Rome, **2**: 1099–1119.

Young, J.R. 1998. Neogene. *In:* P.R. Bown (Ed.). *Calcareous Nannofossil Biostratigraphy*. Kluwer Academic, London: 225–265.

Young, J.R., Bergen, J.A., Bown, P.R., Burnett, J.A., Fiorentino, A., Jordan, R.W., Kleijne, A., van Niel, B.E., *et al*. 1997. Guidelines for coccolith and calcareous nannofossil terminology. *Palaeontology*, **40**(4): 875–912.

# Plate 1

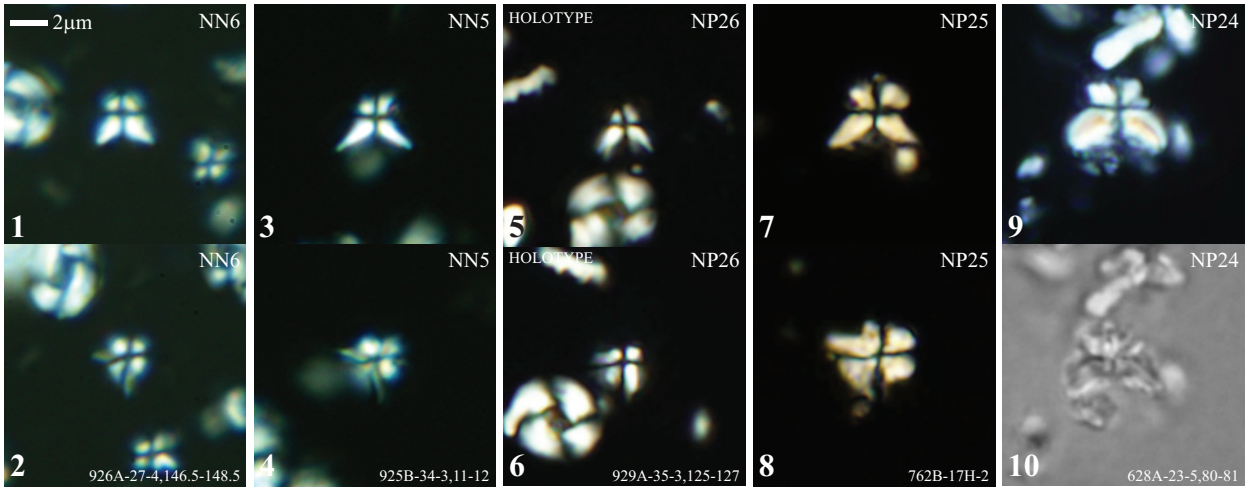


*S. neoabies* *S. neoabies* *S. bipedis* *S. bipedis* *S. bipedis*

*S. bipedis* *S. moriformis* *S. moriformis* *S. moriformis* *S. puniceus*

*S. puniceus* *S. puniceus* *S. puniceus* *S. grandis* *S. grandis*

# Plate 2

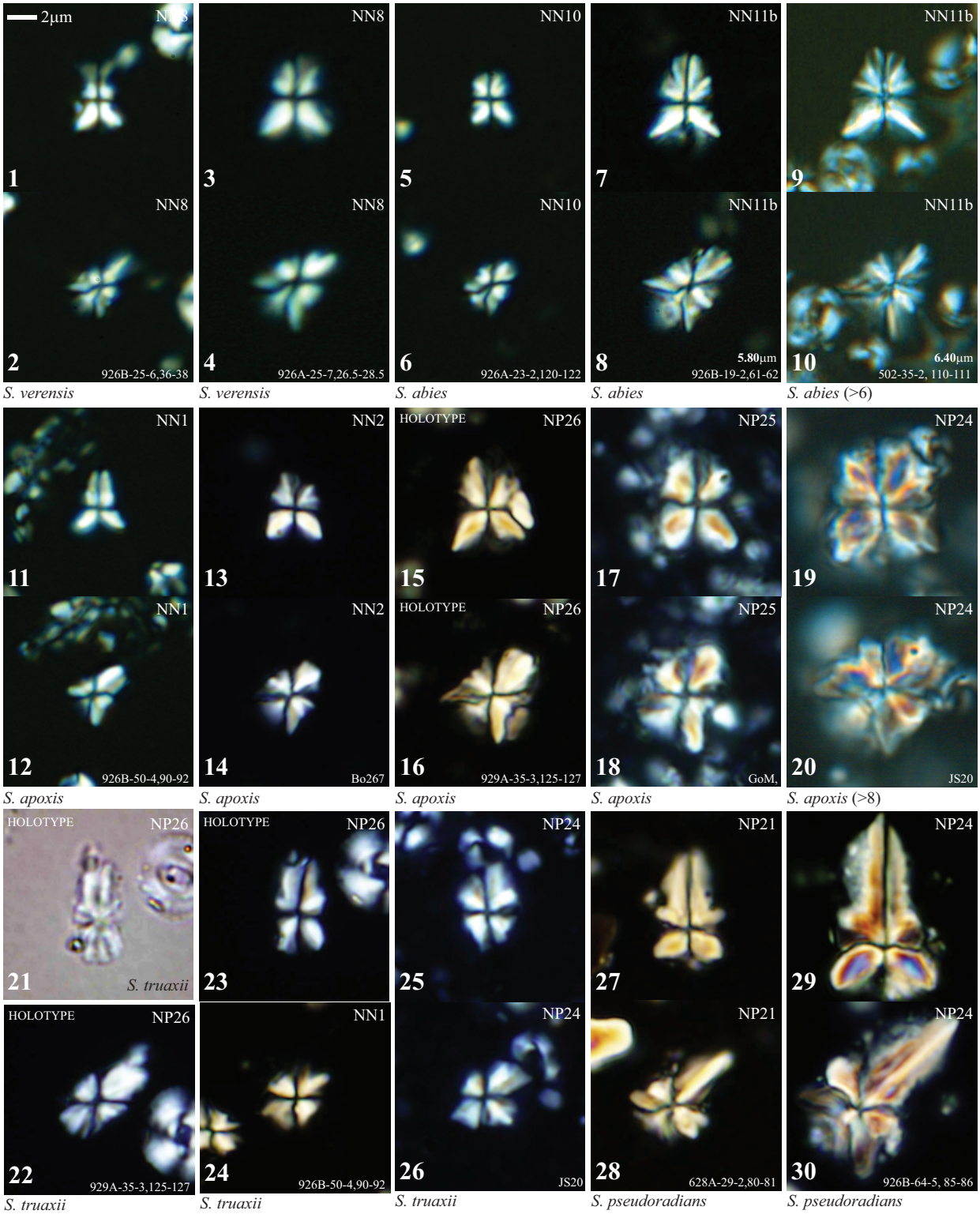
2µm
NN8
1
NN8
2
926B-25-6,36-38
S. verensis
NN8
3
NN8
4
926A-25-7,26.5-28.5
S. verensis
NN10
5
NN10
6
926A-23-2,120-122
S. abies
NN11b
7
NN11b
8
5.80µm
926B-19-2,61-62
S. abies
NN11b
9
NN11b
10
6.40µm
502-35-2, 110-111
S. abies (>6)
NN1
11
NN1
12
926B-50-4,90-92
S. apoxis
NN2
13
NN2
14
Bo267
S. apoxis
HOLOTYPE
NP26
15
HOLOTYPE
NP26
16
929A-35-3,125-127
S. apoxis
NP25
17
NP25
18
GoM,
S. apoxis
NP24
19
NP24
20
JS20
S. apoxis (>8)
HOLOTYPE
NP26
21
S. truaxii
HOLOTYPE
NP26
22
929A-35-3,125-127
S. truaxii
HOLOTYPE
NP26
23
NN1
24
926B-50-4,90-92
S. truaxii
NP24
25
NP24
26
JS20
S. truaxii
NP21
27
NP21
28
628A-29-2,80-81
S. pseudoradians
NP24
29
NP24
30
926B-64-5, 85-86
S. pseudoradians

# Plate 3

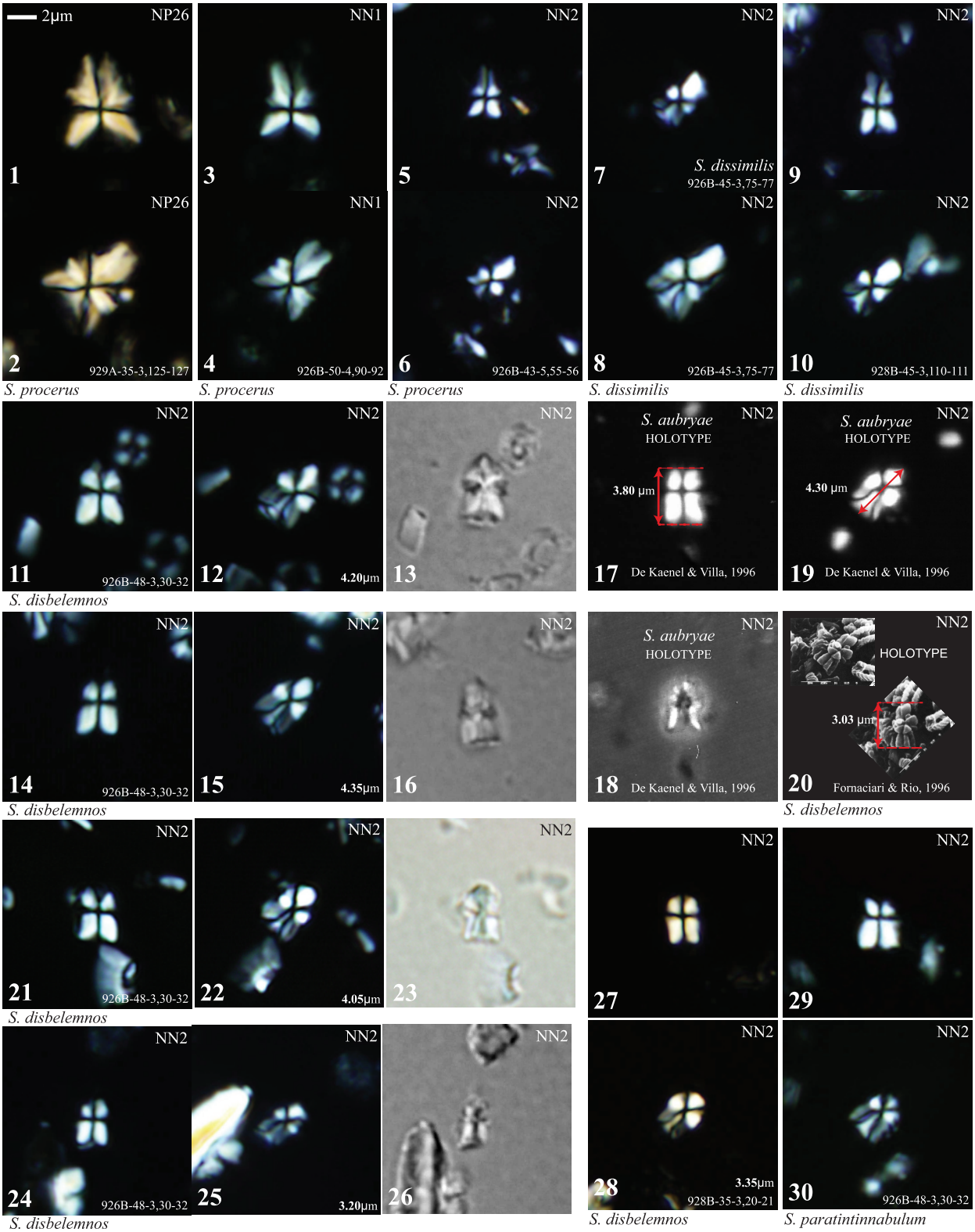
2µm
NP26
1
NN1
3
NN2
5
NN2
7
S. dissimilis
926B-45-3,75-77
NN2
9
NP26
2
929A-35-3,125-127
NN1
4
926B-50-4,90-92
NN2
6
926B-43-5,55-56
NN2
8
926B-45-3,75-77
NN2
10
928B-45-3,110-111
S. procerus
S. procerus
S. procerus
S. dissimilis
S. dissimilis
NN2
11
926B-48-3,30-32
NN2
12
4.20µm
NN2
13
S. aubryae
HOLOTYPE
NN2
3.80 µm
17
De Kaenel & Villa, 1996
S. aubryae
HOLOTYPE
NN2
4.30 µm
19
De Kaenel & Villa, 1996
S. disbelemnos
NN2
14
926B-48-3,30-32
NN2
15
4.35µm
NN2
16
S. aubryae
HOLOTYPE
NN2
18
De Kaenel & Villa, 1996
NN2
HOLOTYPE
3.03 µm
20
Fornaciari & Rio, 1996
S. disbelemnos
S. disbelemnos
NN2
21
926B-48-3,30-32
NN2
22
4.05µm
NN2
23
NN2
27
NN2
29
S. disbelemnos
NN2
24
926B-48-3,30-32
NN2
25
3.20µm
NN2
26
NN2
28
3.35µm
928B-35-3,20-21
NN2
30
926B-48-3,30-32
S. disbelemnos
S. paratintinnabulum

# Plate 4

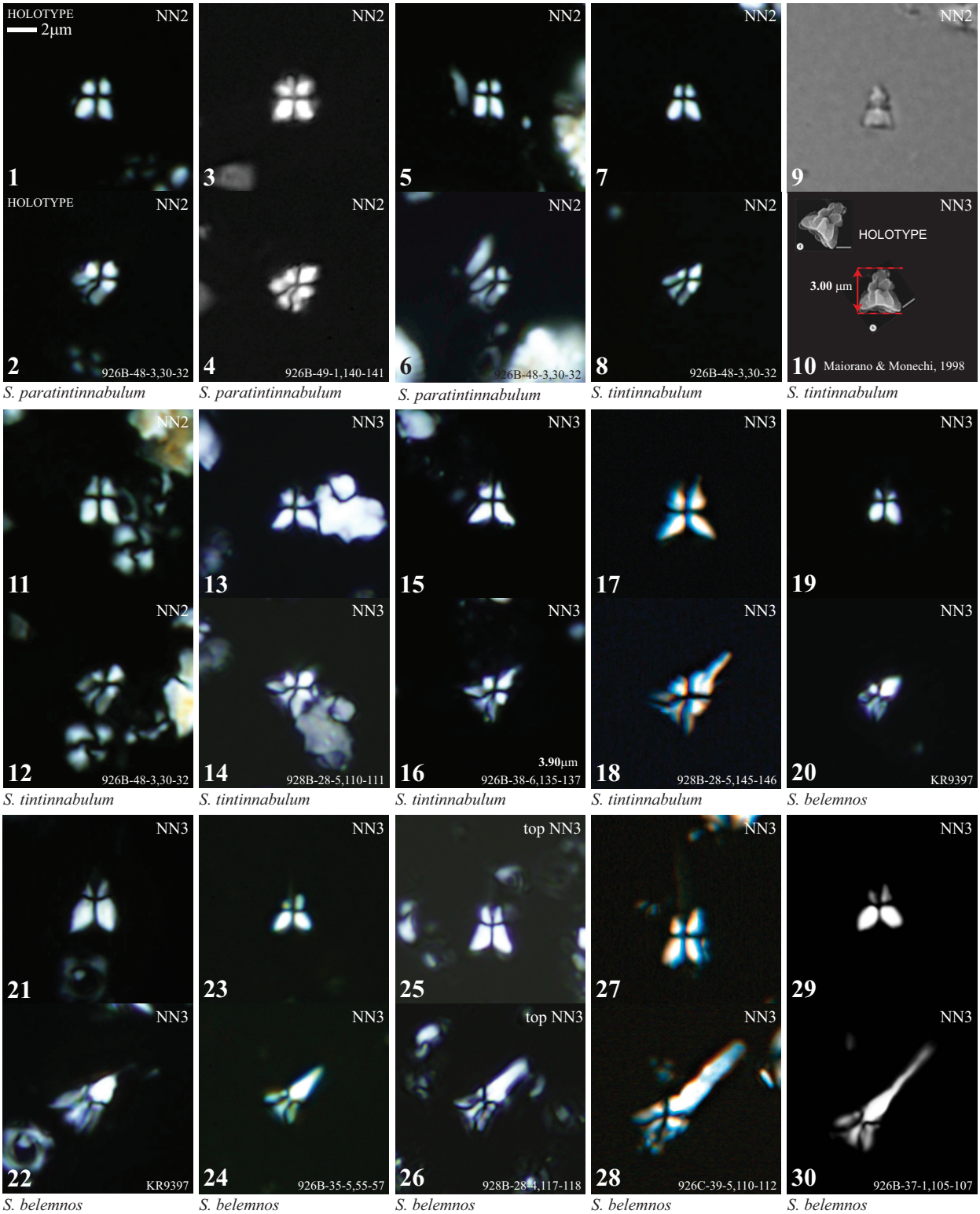
HOLOTYPE
2µm
NN2
1
NN2
3
NN2
5
NN2
7
NN2
9
HOLOTYPE
NN2
2
926B-48-3,30-32
NN2
4
926B-49-1,140-141
NN2
6
926B-48-3,30-32
NN2
8
926B-48-3,30-32
NN3
HOLOTYPE
3.00 µm
10
Maiorano & Monechi, 1998
S. paratintinnabulum
S. paratintinnabulum
S. paratintinnabulum
S. tintinnabulum
S. tintinnabulum
NN2
11
NN3
13
NN3
15
NN3
17
NN3
19
NN2
12
926B-48-3,30-32
NN3
14
928B-28-5,110-111
NN3
3.90µm
16
926B-38-6,135-137
NN3
18
928B-28-5,145-146
NN3
20
KR9397
S. tintinnabulum
S. tintinnabulum
S. tintinnabulum
S. tintinnabulum
S. belemnos
NN3
21
NN3
23
top NN3
25
NN3
27
NN3
29
NN3
22
KR9397
NN3
24
926B-35-5,55-57
top NN3
26
928B-28-4,117-118
NN3
28
926C-39-5,110-112
NN3
30
926B-37-1,105-107
S. belemnos
S. belemnos
S. belemnos
S. belemnos
S. belemnos

# Plate 5

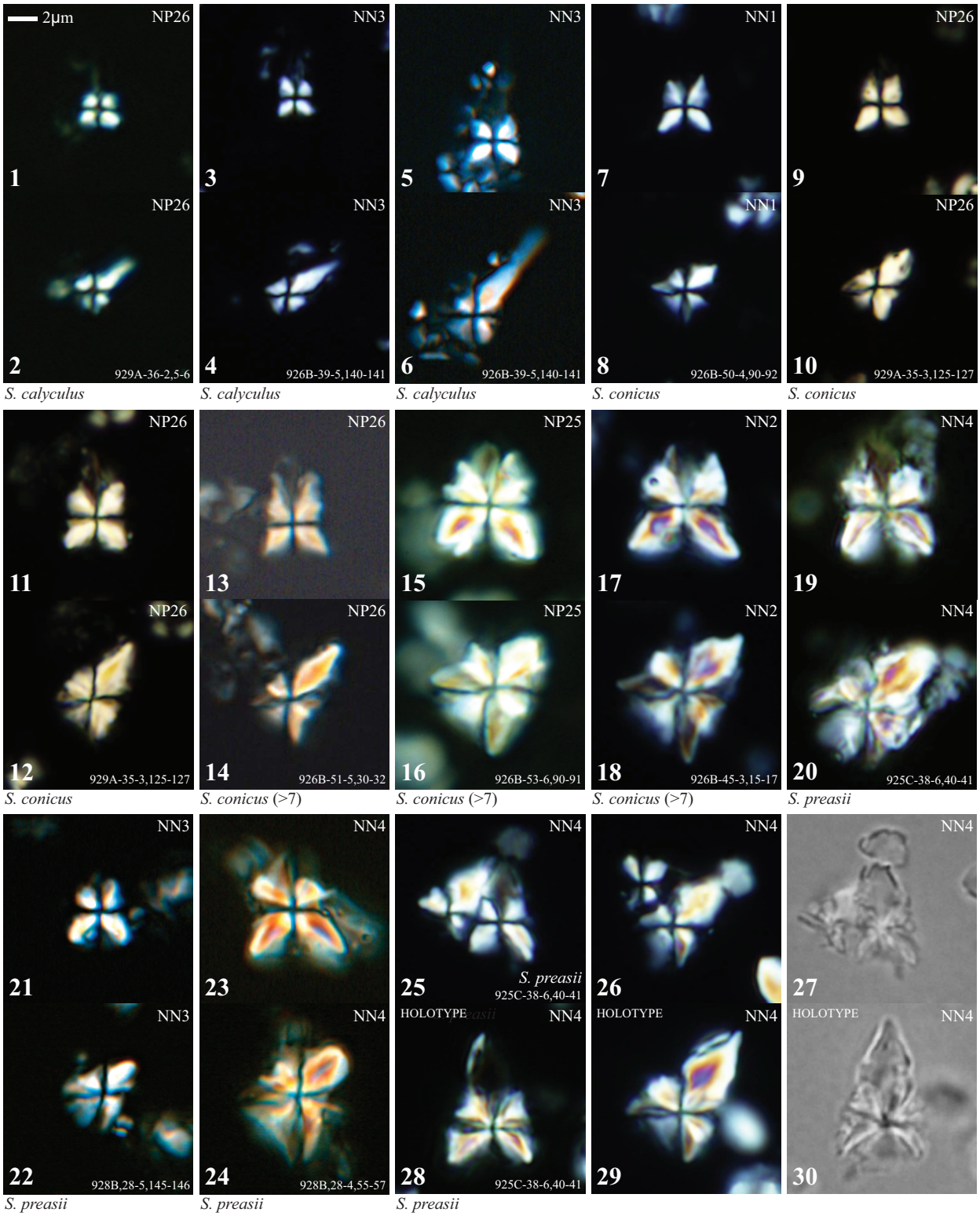
2µm
NP26
1
NP26
2
929A-36-2,5-6
S. calyculus
NN3
3
NN3
4
926B-39-5,140-141
S. calyculus
NN3
5
NN3
6
926B-39-5,140-141
S. calyculus
NN1
7
NN1
8
926B-50-4,90-92
S. conicus
NP26
9
NP26
10
929A-35-3,125-127
S. conicus
NP26
11
NP26
12
929A-35-3,125-127
S. conicus
NP26
13
NP26
14
926B-51-5,30-32
S. conicus (>7)
NP25
15
NP25
16
926B-53-6,90-91
S. conicus (>7)
NN2
17
NN2
18
926B-45-3,15-17
S. conicus (>7)
NN4
19
NN4
20
925C-38-6,40-41
S. preasii
NN3
21
NN3
22
928B,28-5,145-146
S. preasii
NN4
23
NN4
24
928B,28-4,55-57
S. preasii
NN4
25
S. preasii
925C-38-6,40-41
HOLOTYPE
NN4
28
925C-38-6,40-41
S. preasii
NN4
26
HOLOTYPE
NN4
29
NN4
27
HOLOTYPE
NN4
30

# Plate 6

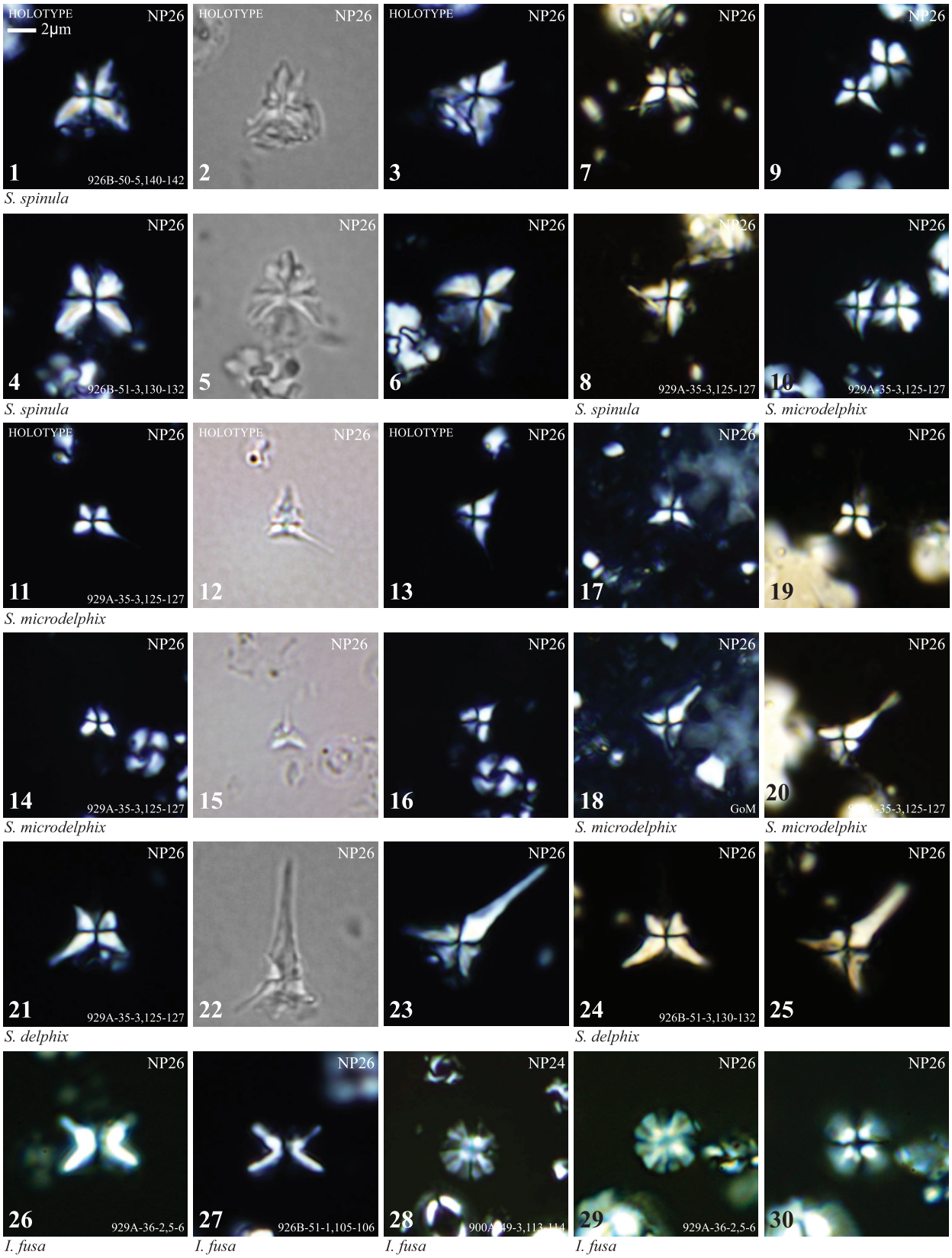


*S. spinula* *S. spinula* *S. spinula* *S. microdelphix*

*S. microdelphix* *S. microdelphix* *S. microdelphix*

*S. delphix* *S. delphix*

*I. fusa* *I. fusa* *I. fusa* *I. fusa*

# Plate 7

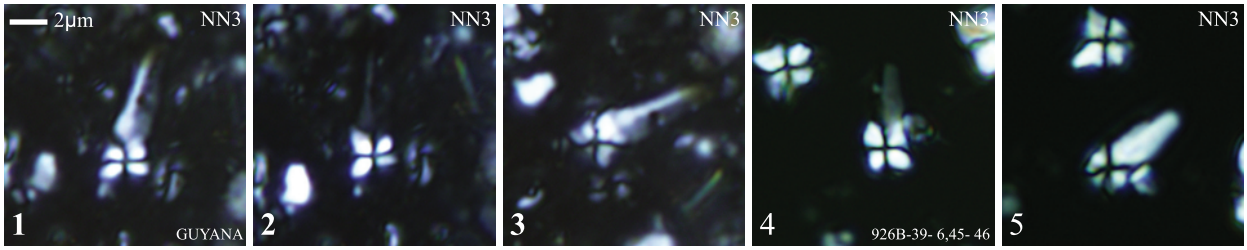


*S. pseudoheteromorphus* *S. pseudoheteromorphus*

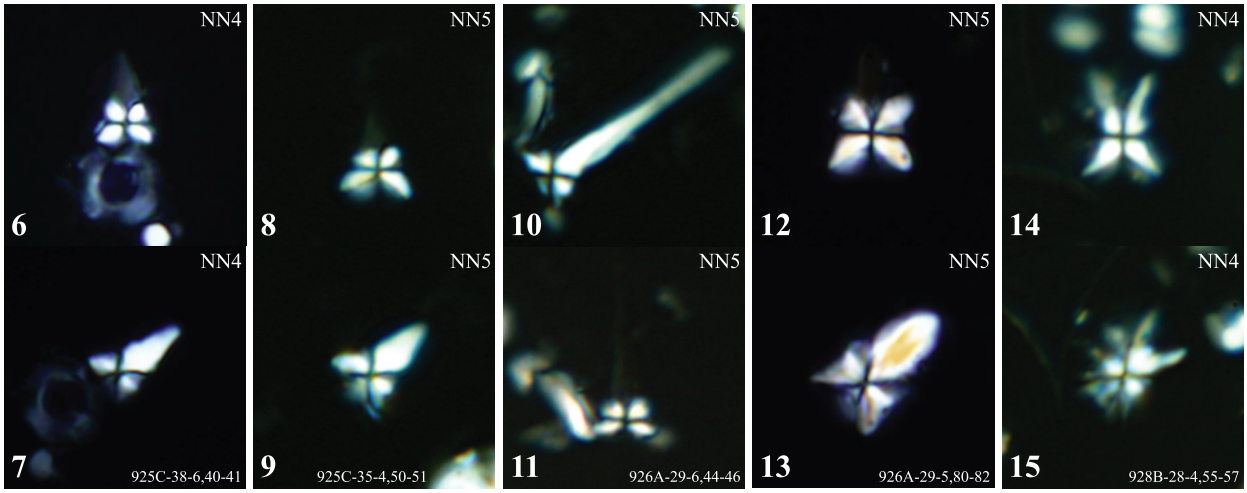


*S. heteromorphus* *S. heteromorphus* *S. heteromorphus* *S. heteromorphus* (trans) *S. multispinatus*

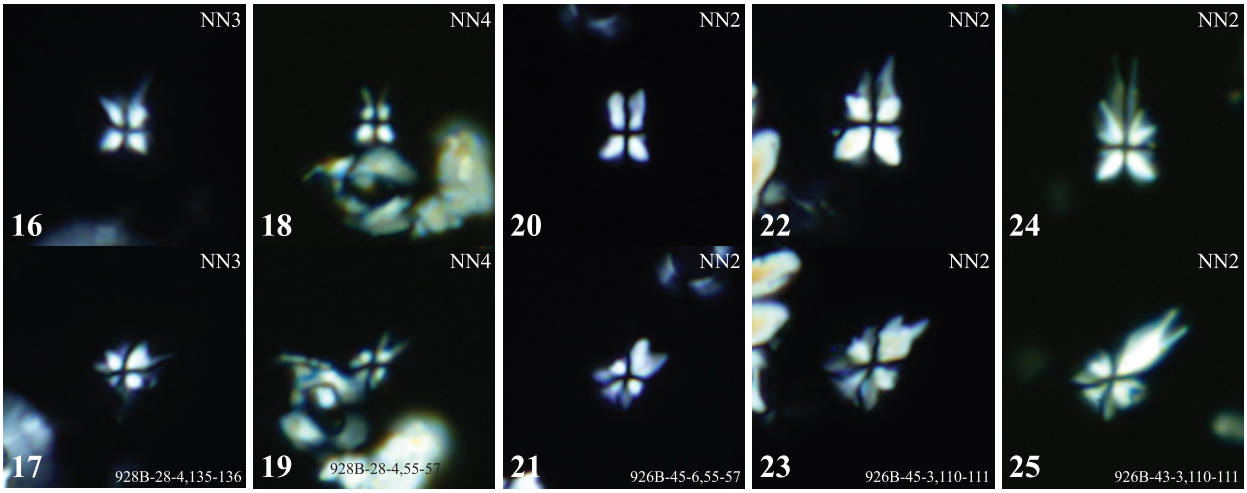


*S. multispinatus* *S. cometa* *S. cometa* *S. cometa* *S. cometa*

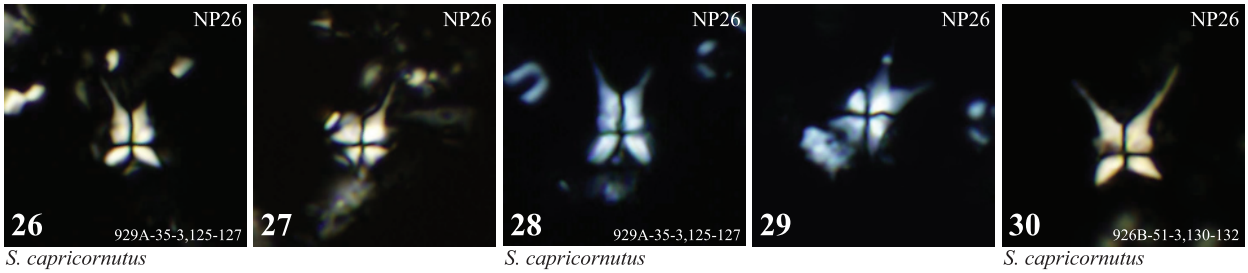


*S. capricornutus* *S. capricornutus* *S. capricornutus*

# Plate 8

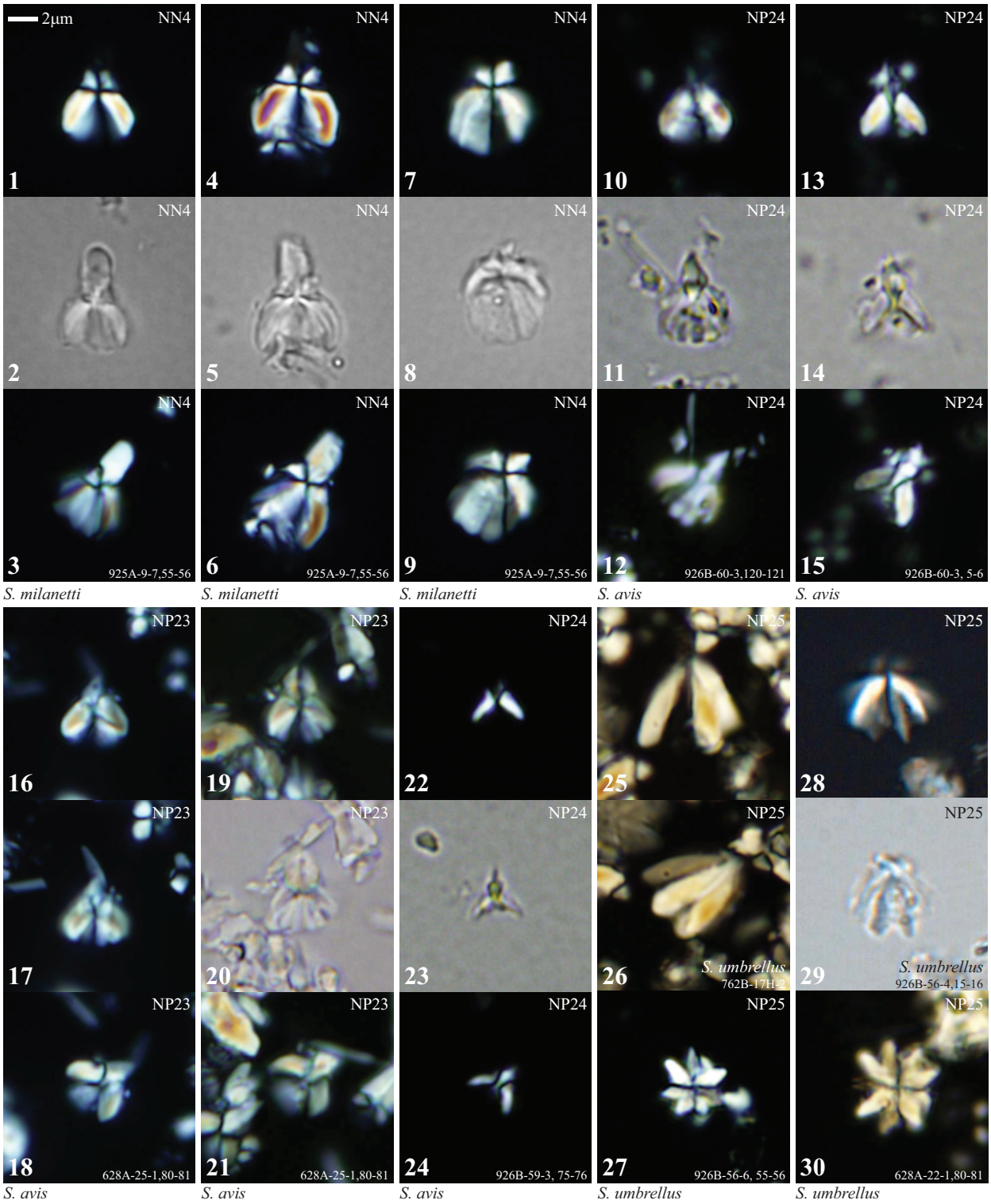
2µm
NN4
1
NN4
4
NN4
7
NP24
10
NP24
13
NN4
2
NN4
5
NN4
8
NP24
11
NP24
14
NN4
3
925A-9-7,55-56
NN4
6
925A-9-7,55-56
NN4
9
925A-9-7,55-56
NP24
12
926B-60-3,120-121
NP24
15
926B-60-3, 5-6
S. milanetti
S. milanetti
S. milanetti
S. avis
S. avis
NP23
16
NP23
19
NP24
22
NP25
25
NP25
28
NP23
17
NP23
20
NP24
23
NP25
26
S. umbrellus
762B-17H-2
NP25
29
S. umbrellus
926B-56-4,15-16
NP23
18
628A-25-1,80-81
NP23
21
628A-25-1,80-81
NP24
24
926B-59-3, 75-76
NP25
27
926B-56-6, 55-56
NP25
30
628A-22-1,80-81
S. avis
S. avis
S. avis
S. umbrellus
S. umbrellus

# Plate 9

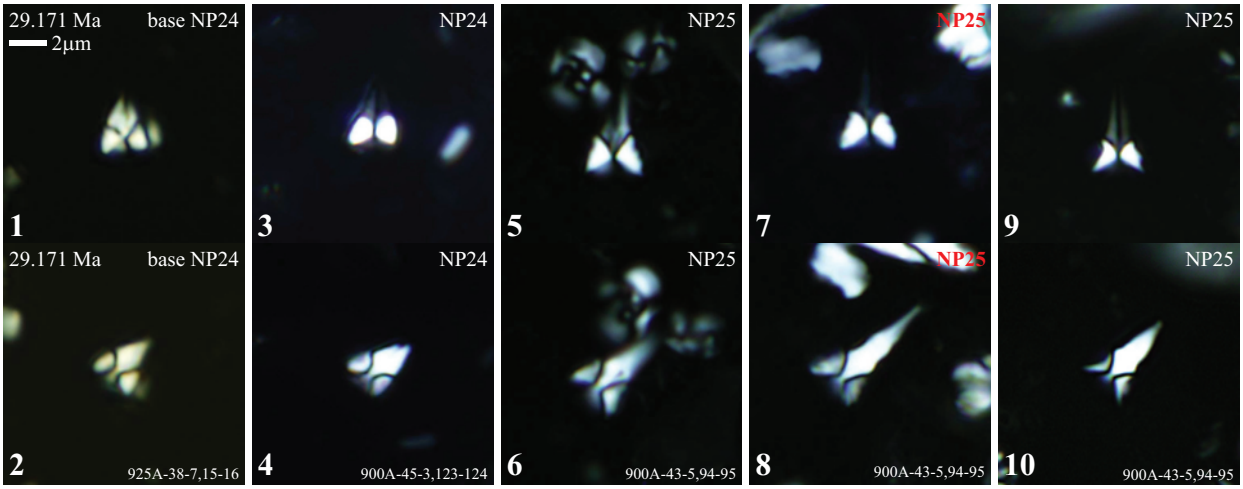


*S. ciperoensis* | *S. ciperoensis* | *S. ciperoensis* | *S. ciperoensis* (>6) | *S. patifunditus*

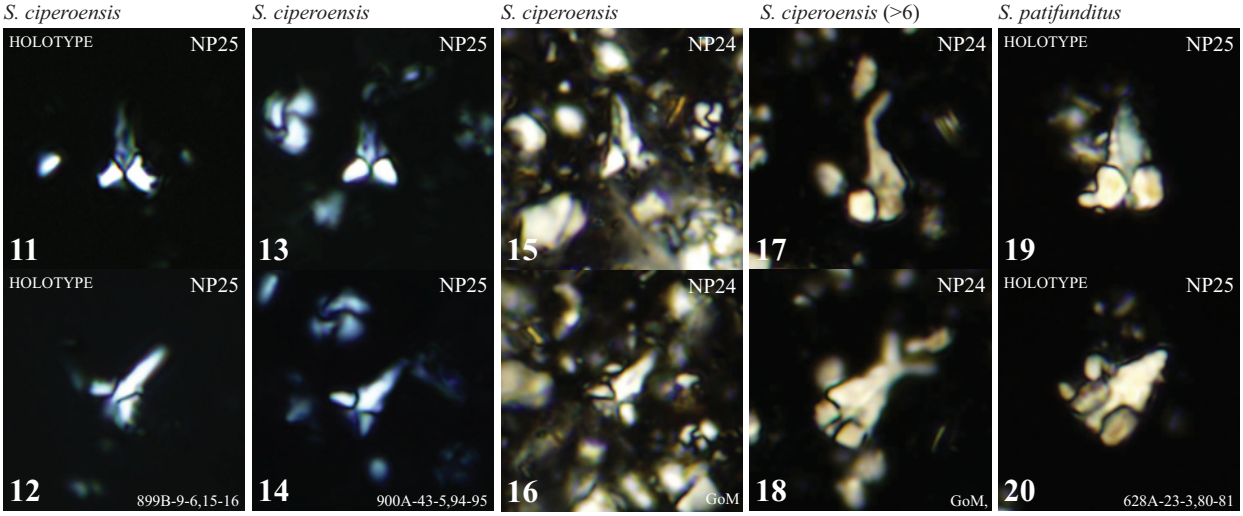


*S. patifunditus* | *S. patifunditus* | *S. patifunditus* | *S. tawfikii* | *S. tawfikii*

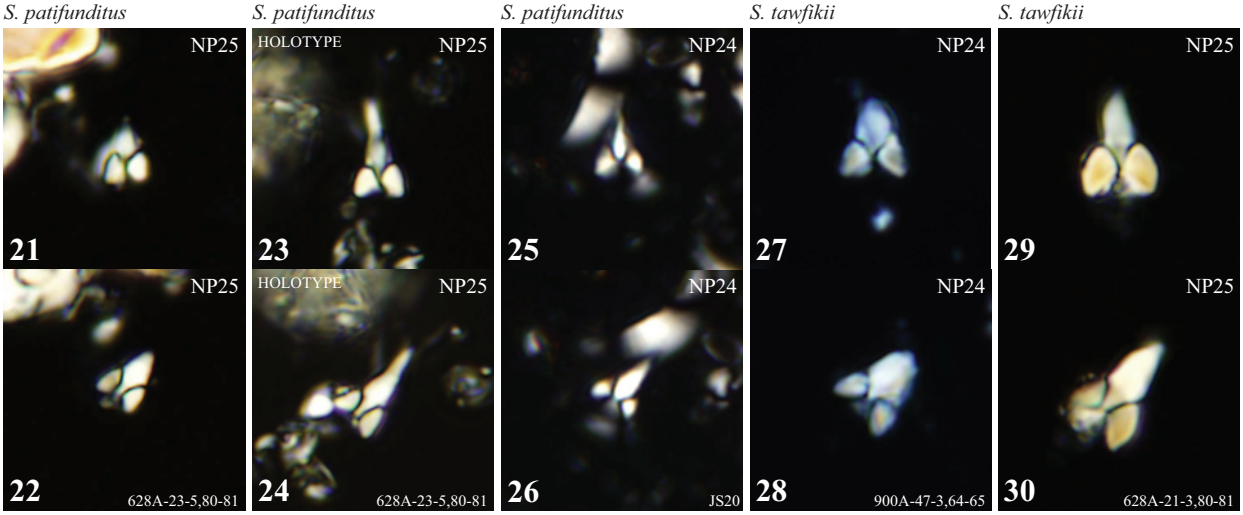


*S. directus* | *S. directus* | *S. bulbulus* | *S. bulbulus* | *S. bulbulus*

# Plate 10

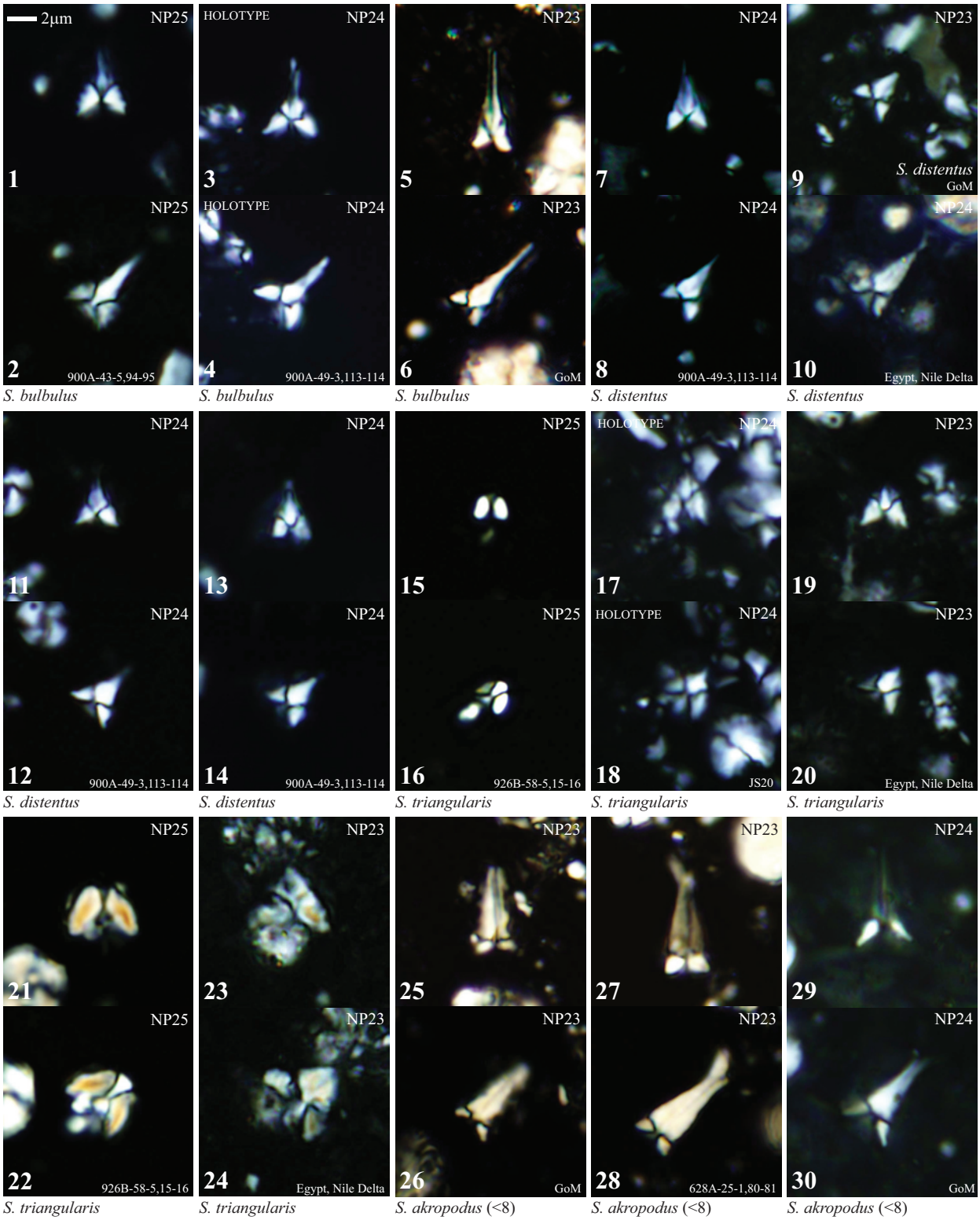
2µm
NP25
1
NP25
2
900A-43-5,94-95
S. bulbulus
HOLOTYPE
NP24
3
HOLOTYPE
NP24
4
900A-49-3,113-114
S. bulbulus
NP23
5
NP23
6
GoM
S. bulbulus
NP24
7
NP24
8
900A-49-3,113-114
S. distentus
NP23
9
S. distentus
GoM
NP24
10
Egypt, Nile Delta
S. distentus
NP24
11
NP24
12
900A-49-3,113-114
S. distentus
NP24
13
NP24
14
900A-49-3,113-114
S. distentus
NP25
15
NP25
16
926B-58-5,15-16
S. triangularis
HOLOTYPE
NP24
17
HOLOTYPE
NP24
18
JS20
S. triangularis
NP23
19
NP23
20
Egypt, Nile Delta
S. triangularis
NP25
21
NP25
22
926B-58-5,15-16
S. triangularis
NP23
23
NP23
24
Egypt, Nile Delta
S. triangularis
NP23
25
NP23
26
GoM
S. akropodus (<8)
NP23
27
NP23
28
628A-25-1,80-81
S. akropodus (<8)
NP24
29
NP24
30
GoM
S. akropodus (<8)

# Plate 11

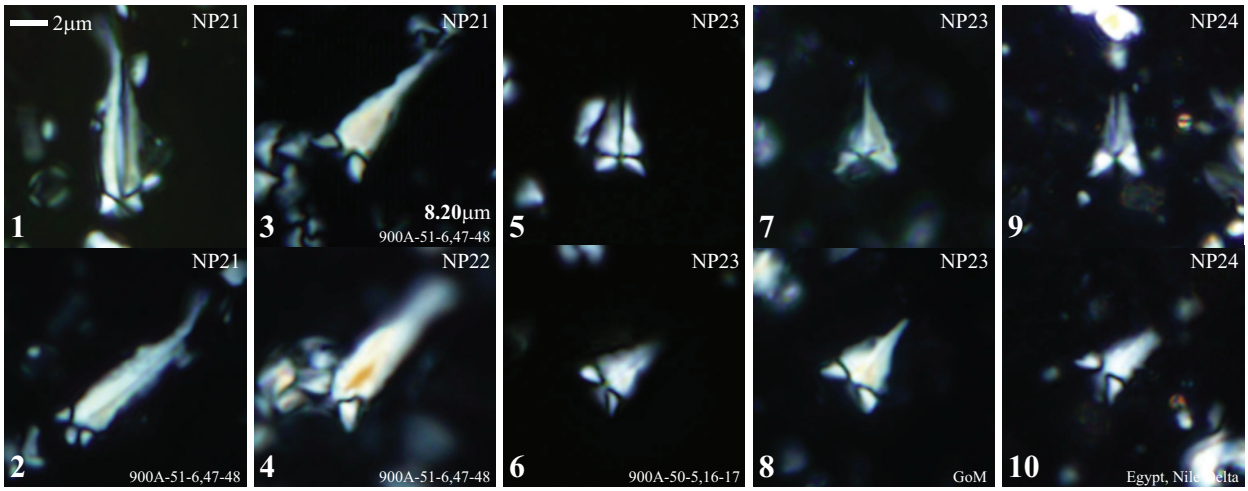


*S. akropodus* | *S. akropodus* | *S. peartiae* | *S. peartiae* | *S. peartiae*

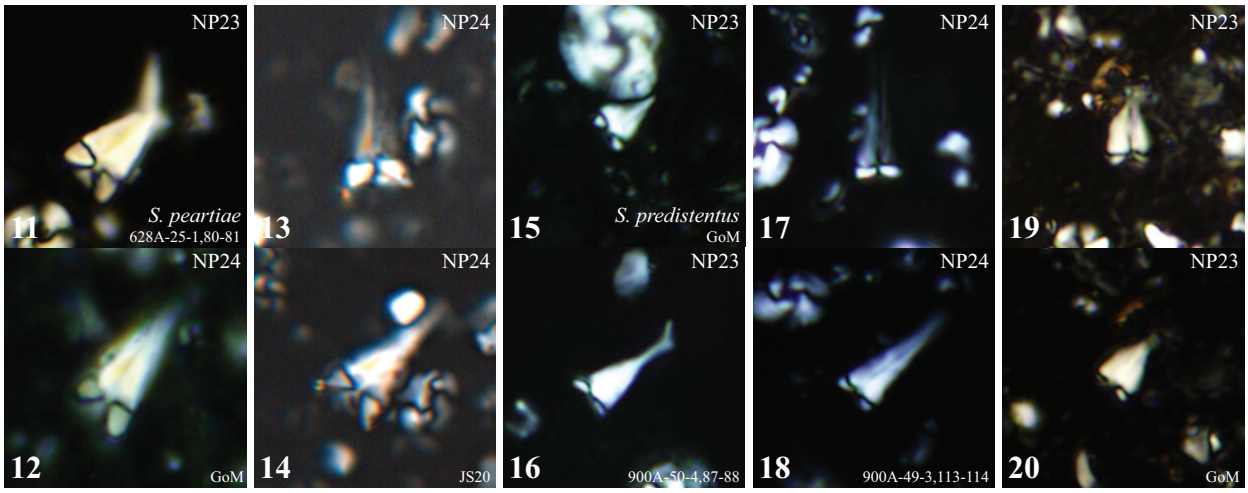


*S. peartiae* (>7) | *S. peartiae* (>7) | *S. predistentus* (trans) | *S. predistentus* | *S. predistentus*

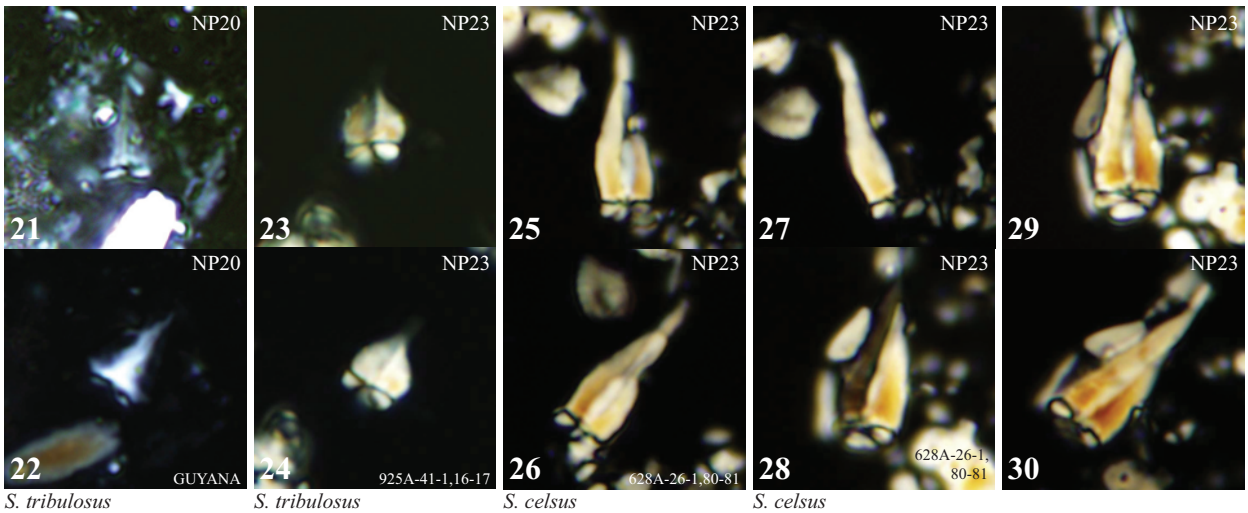


*S. tribulosus* | *S. tribulosus* | *S. celsus* | *S. celsus*